NATIONAL ADVISORY COMMITTEE FOR AERONAUTICS

REPORT No. 379

ROLLING MOMENTS DUE TO ROLLING AND YAW FOR FOUR WING MODELS IN ROTATION

By MONTGOMERY KNIGHT and CARL J. WENZINGER

1931

For sale by the Superintendent of Documents, Washington, D. C. - - - - - - - - - Price 15 cents

AERONAUTICAL SYMBOLS

1. FUNDAMENTAL AND DERIVED UNITS

	Symbol	Metric		English	
		Unit	Symbol	Unit	Symbol
Length	l	meter	m	foot (or mile)	ft. (or mi.)
Time	t	second	s	second (or hour)	sec. (or hr.)
Force	F	weight of one kilogram	kg	weight of one pound	lb.
Power	P	kg/m/s		horsepower	hp
Speed		km/h	k. p. h.	mi./hr.	m. p. h.
		m/s	m. p. s.	ft./sec.	f. p. s.

2. GENERAL SYMBOLS, ETC.

W, Weight $= mg$

g, Standard acceleration of gravity $= 9.80665$ m/s^2 $= 32.1740$ ft./sec.^{2}

m, Mass $= \frac{W}{g}$

ρ, Density (mass per unit volume).

Standard density of dry air, 0.12497 (kg-m^{-4} s^2) at 15° C. and 750 mm $= 0.002378$ (lb.-ft.$^{-4}$ sec.^{2}).

Specific weight of "standard" air, 1.2255 kg/m^3 $= 0.07651$ lb./ft.^{3}.

mk^2, Moment of inertia (indicate axis of the radius of gyration k, by proper subscript).

S, Area.

S_w, Wing area, etc.

G, Gap.

b, Span.

c, Chord.

$\frac{b^2}{S}$, Aspect ratio.

μ, Coefficient of viscosity.

3. AERODYNAMICAL SYMBOLS

V, True air speed.

q, Dynamic (or impact) pressure $= \frac{1}{2}\rho V^2$.

L, Lift, absolute coefficient $C_L = \frac{L}{qS}$

D, Drag, absolute coefficient $C_D = \frac{D}{qS}$

D_o, Profile drag, absolute coefficient $C_{D_o} = \frac{D_o}{qS}$

D_i, Induced drag, absolute coefficient $C_{D_i} = \frac{D_i}{qS}$

D_p, Parasite drag, absolute coefficient $C_{D_p} = \frac{D_p}{qS}$

C, Cross-wind force, absolute coefficient $C_C = \frac{C}{qS}$

R, Resultant force.

i_w, Angle of setting of wings (relative to thrust line).

i_t, Angle of stabilizer setting (relative to thrust line).

Q, Resultant moment.

Ω, Resultant angular velocity.

$\rho\frac{Vl}{\mu}$, Reynolds Number, where l is a linear dimension.

e. g., for a model airfoil 3 in. chord, 100 mi./hr. normal pressure, at 15° C., the corresponding number is 234,000;

or for a model of 10 cm chord 40 m/s, the corresponding number is 274,000.

C_p, Center of pressure coefficient (ratio of distance of c. p. from leading edge to chord length).

α, Angle of attack.

ϵ, Angle of downwash.

α_o, Angle of attack, infinite aspect ratio.

α_i, Angle of attack, induced.

α_a, Angle of attack, absolute.

(Measured from zero lift position.)

γ, Flight path angle.

REPORT No. 379

ROLLING MOMENTS DUE TO ROLLING AND YAW FOR FOUR WING MODELS IN ROTATION

By MONTGOMERY KNIGHT and CARL J. WENZINGER
Langley Memorial Aeronautical Laboratory

35387—31——1

NATIONAL ADVISORY COMMITTEE FOR AERONAUTICS

NAVY BUILDING, WASHINGTON, D. C.

(An independent Government establishment, created by act of Congress approved March 3, 1915, for the supervision and direction of the scientific study of the problems of flight. Its membership was increased to 15 by act approved March 2, 1929 (Public, No. 908, 70th Congress). It consists of members who are appointed by the President, all of whom serve as such without compensation.)

EXECUTIVE COMMITTEE

REPORT NO. 379

ROLLING MOMENTS DUE TO ROLLING AND YAW FOR FOUR WING MODELS IN ROTATION

By MONTGOMERY KNIGHT and CARL J. WENZINGER

SUMMARY

This report presents the results of a series of autorotation and torque tests on four different rotating wing systems at various rates of roll and at several angles of yaw. The investigation covered an angle-of-attack range up to 90° and angles of yaw of 0°, 5°, 10°, and 20°. The tests were made in the 5-foot, closed-throat atmospheric wind tunnel of the National Advisory Committee for Aeronautics. The object of the tests was primarily to determine the effects of various angles of yaw on the rolling moments of the rotating wings up to large angles of attack.

It was found that at angles of attack above that of maximum lift the rolling moments on the wings due to yaw (or side slip) from 5° to 20° were roughly of the same magnitude as those due to rolling. There was a wide variation in magnitude of the rolling moment due to yaw angle with both angle of attack and with $\frac{pb}{2V}$. *The rates and ranges of stable autorotation for the monoplane models were considerably increased by yaw, whereas for an unstaggered biplane they were little affected. The immediate cause of the rolling moment due to yaw is apparently the building up of large loads on the forward wing tip and the reduction of loads on the rearward wing tip.*

INTRODUCTION

The rotational motion which is characteristic of the spin of an airplane is due chiefly to certain rolling moments produced by the wings. These moments arise as the result of three principal causes:

1. The rotational motion itself.
2. The angle of yaw or side slip.
3. The ailerons.

The rolling moment due to the angular velocity in roll has until recently been thought of as the primary cause of the spin. It has been the subject of a number of wind-tunnel and mathematical investigations such as the one given in Reference 1. The mathematical analyses have been based upon the "strip method" of determining the rolling moments due to rolling for various wing systems.

Certain investigations have indicated that an additional large rolling moment is produced at angles of attack beyond that of maximum lift when a wing is given an angular displacement in yaw. That this moment exists when the wing is stationary is shown in References 2, 3, 4, and 5, and some of the anomalous effects produced by it in the case of certain airplanes in stalled flight are indicated in References 6 and 7. Chief of the effects due to yaw and to yawing (References 6 and 7) is the apparent reversal of aileron control, since at large angles of attack the instrumental records show that the ultimate roll is in a direction opposite to that which the ailerons would normally produce. The rolling moment due to yaw also persists when the wing is rotating, as is shown in References 8 and 9, which describe wind-tunnel investigations wherein the models were free to rotate about a central axis parallel to the wind direction. This fact is indicated by the increased rates and angular ranges of stable autorotation which obtained when the models were given an angle of yaw.

The present report does not include a study of the variation in aileron characteristics with yaw and rate of roll, since it was necessary to limit the variables in order to complete the tests within a reasonable length of time. This phase of the subject is partially covered in References 10 and 11.

So far as the writers have been able to ascertain, no tests had previously been made in which rolling moments were measured on a rotating wing at various angles of yaw. The object of this wind-tunnel investigation, which was conducted at the Langley Memorial Aeronautical Laboratory, was to supply such information. A partial explanation is given of the relatively large rolling moments due to yaw occurring at large angles of attack.

The tests were made in the 5-foot atmospheric wind tunnel (Reference 12) on models of four representative wing systems: namely, an unstaggered biplane and three different monoplane wings. The rolling moments were measured on a small electric dynamometer designed especially for the purpose. A large range of angles of attack was covered.

MODELS AND APPARATUS

The models used consisted of one biplane and three different monoplane wings. The biplane had zero

stagger and a gap/chord ratio of 1.0. Both upper and lower wings had a 5-inch chord and were of aspect ratio 6. The tips were circular and the Clark Y profile was used. Figure 1 shows the general arrangement of this model. One wing of the biplane was also tested as a monoplane wing, and is shown as such in Figure 2.

The second monoplane-wing model had the N. A. C. A. 84 profile, but was rectangular in plan form except for the tips. These were faired, as shown in the diagram of the wing, Figure 3. The model also had a 5-inch chord and an aspect ratio of 6.

The third monoplane-wing model was designated as the N. A. C. A. 86–M and was tapered in plan

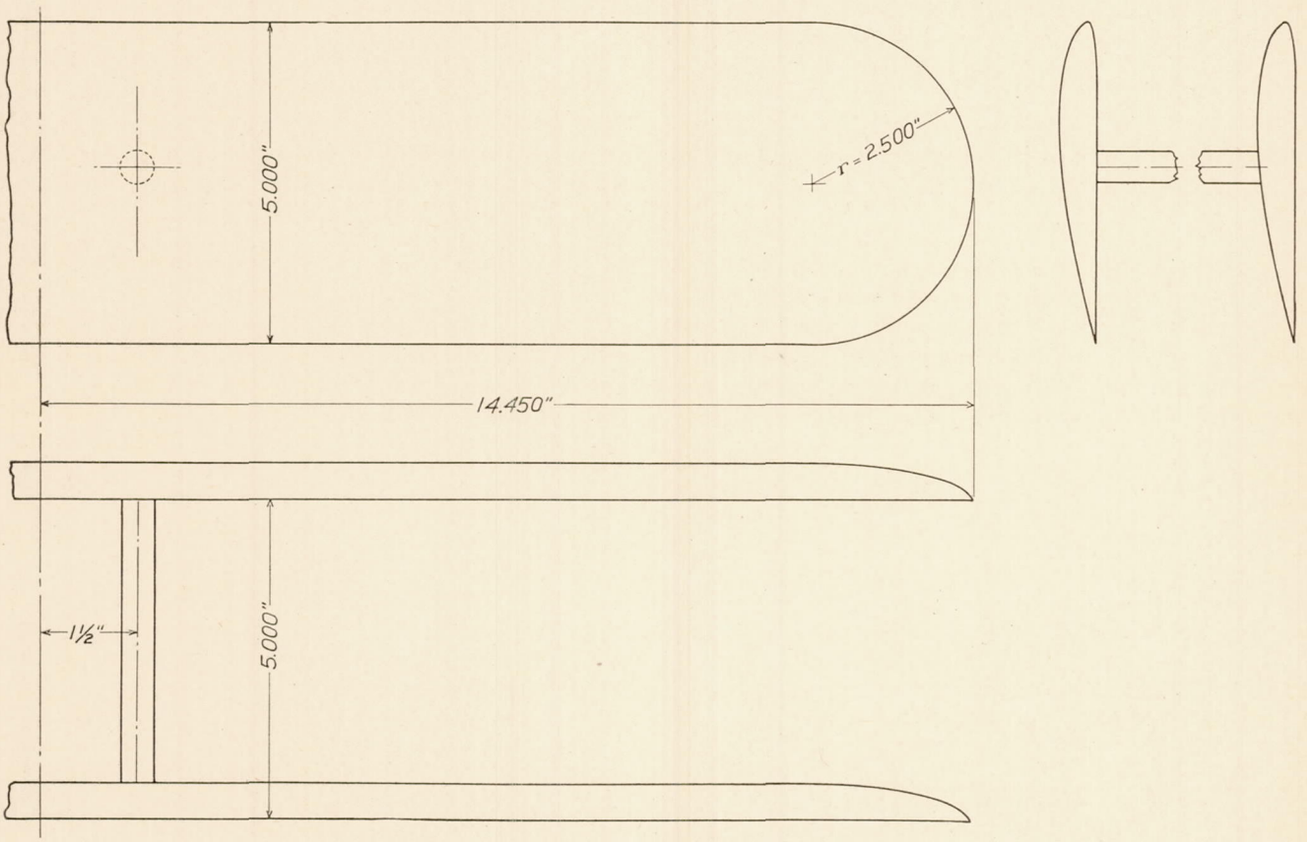

FIGURE 1.—Biplane wing model—Clark Y

and thickness, having a ratio of tip chord to root chord of 0.5. The N. A. C. A. 84 profile was used at the root section and the N. A. C. A.–M2 profile at the tips, which were circular in plan. The model had an aspect ratio of 6, and is shown in Figure 4.

All of the models were made of laminated mahogany. In the construction of the models the profile ordinates were held accurate to within ±0.003 inch of those listed in Tables I, II, and III.

The autorotation dynamometer consists essentially of a shaft parallel to the air stream and rotating on ball bearings. It is driven through reduction gearing by a small, direct-current motor mounted in a cradle on knife-edges. (See fig. 5.)

An arm attached to the cradle at right angles to the knife edges transmits the torques to a balance outside of the tunnel (fig. 6), upon which the rolling moments for rotations in either direction are measured. The dynamometer assembly is housed in an aluminum fairing, as shown in Figure 7, which is a view of the installation in the 5-foot closed-throat atmospheric wind tunnel.

The wing was mounted on the dynamometer-shaft extension arm, as shown. A simple clamp arrangement on the model, and the angle-of-attack changing mechanism outside the tunnel (fig. 8) permitted the angle of attack to be varied as desired. The rate and direction of rotation were controlled by a variable-speed motor with a reversing switch, used in conjunction with a stroboscopic tachometer and stop watch. The angle of yaw was adjusted by clamping the model at the desired position on its supporting arm, using an inclinometer placed on the leading edge to indicate the angle.

TESTS

Before making the actual autorotation tests on the various models a few preliminary tests were made for calibration purposes. With the dynamometer in place, but without any model mounted on the extension arm, vertical velocity surveys were made at approximately the location of the model. A Pitot-static tube, installed permanently in the tunnel sufficiently far upstream from the model to be unaffected by it, was then cali-

brated against the integrated mean of the final survey and used as a dynamic pressure reference.

Tare rolling-moment tests were then made to determine the magnitude of the effects due to the ball-bearing friction and windage of the model support arm. With the tunnel operating, the arm was driven by the dynamometer motor at speeds ranging from 0 to 500 r. p. m., and the rolling moments were measured at several points for rotations in both positive and negative directions. Curves were then plotted, and from these the total rolling moments due to the models were corrected.

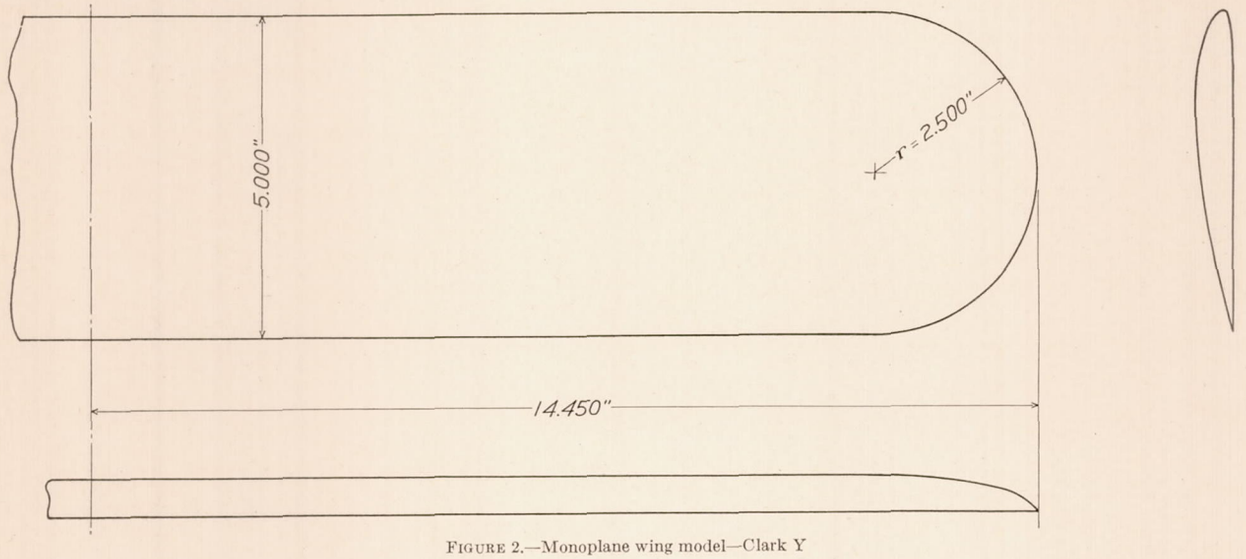

FIGURE 2.—Monoplane wing model—Clark Y

The tests on each wing model were made in two parts:

1. Stable autorotation tests.
2. Rolling moment tests.

In general the angle-of-attack range was from 0° to 90°, and angles of yaw were set at 0°, 5°, 10°, and 20°. Rotations of the models were varied between 0 and 500 r. p. m. and were taken in both positive and negative directions. The tests were made on three of the models at a dynamic pressure of 4.05 pounds per square foot, corresponding to an average air speed of 39.8 m. p. h. For comparison with pressure-distribution tests the dynamic pressure was maintained at 5.01 pounds per square foot for the tests on the N. A. C. A. 84 wing model, since a slight scale effect was found to exist at the two different pressures.

When making the stable autorotation tests, the model was allowed to rotate freely by merely disengaging the reduction gearing in the dynamometer. The rates of rotation in both directions at various angles of attack were measured by counting the revolutions for a period of time. In addition the angles of attack between which the model would start rotating of itself, and also those at which it did not quite rotate when given a start by hand, were observed.

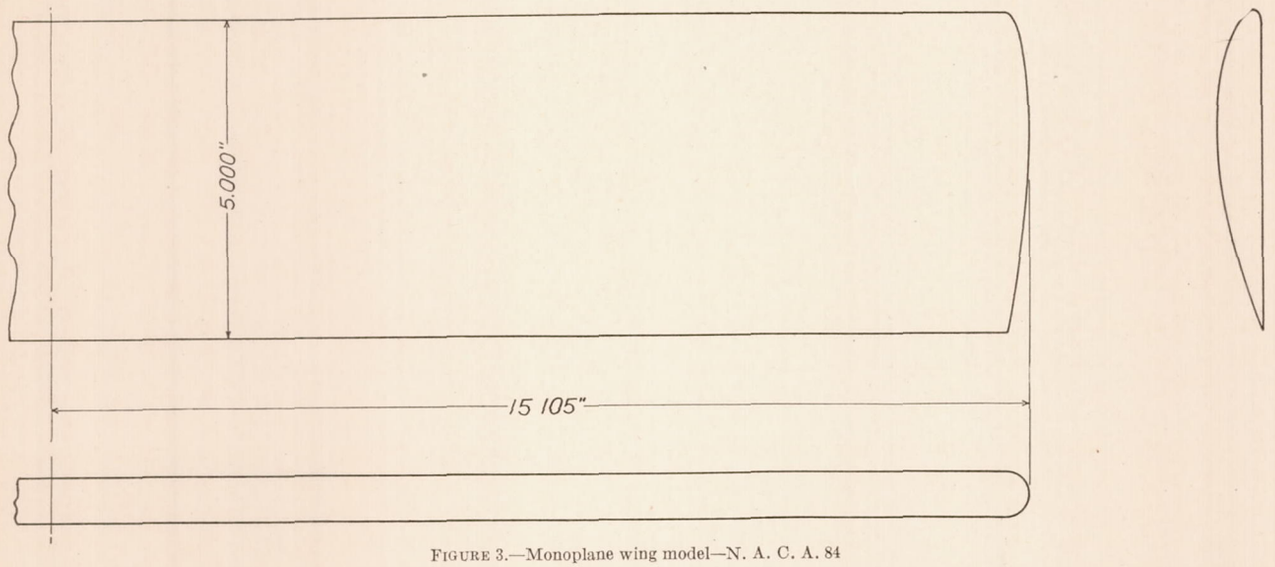

FIGURE 3.—Monoplane wing model—N. A. C. A. 84

The rolling-moment tests were made with the dynamometer gearing in mesh, so that the speed of rotation was controlled by the motor. Static moments were first measured with the tunnel operating, and then not operating, for the model both in the normal position of flight and then inverted. Moments due to

the rotation were obtained for both directions at various rates and angles of attack. Rotation of the model was measured by counting the revolutions for a period of time for low rates of rotation and by use of the stroboscopic tachometer for the higher rates.

As the result of check tests, the probable accuracy obtained in the investigation was estimated as follows:

(*a*) Angle-of-attack setting—$\pm 0.2°$.
(*b*) Angle-of-yaw setting—$\pm 0.2°$.
(*c*) Rolling-moment balance—± 0.5 gram.
(*d*) R. p. m. measurements—± 1.0 per cent.
(*e*) Dynamic pressure—± 0.75 per cent.
(*f*) Data as tabulated—± 3.0 per cent.

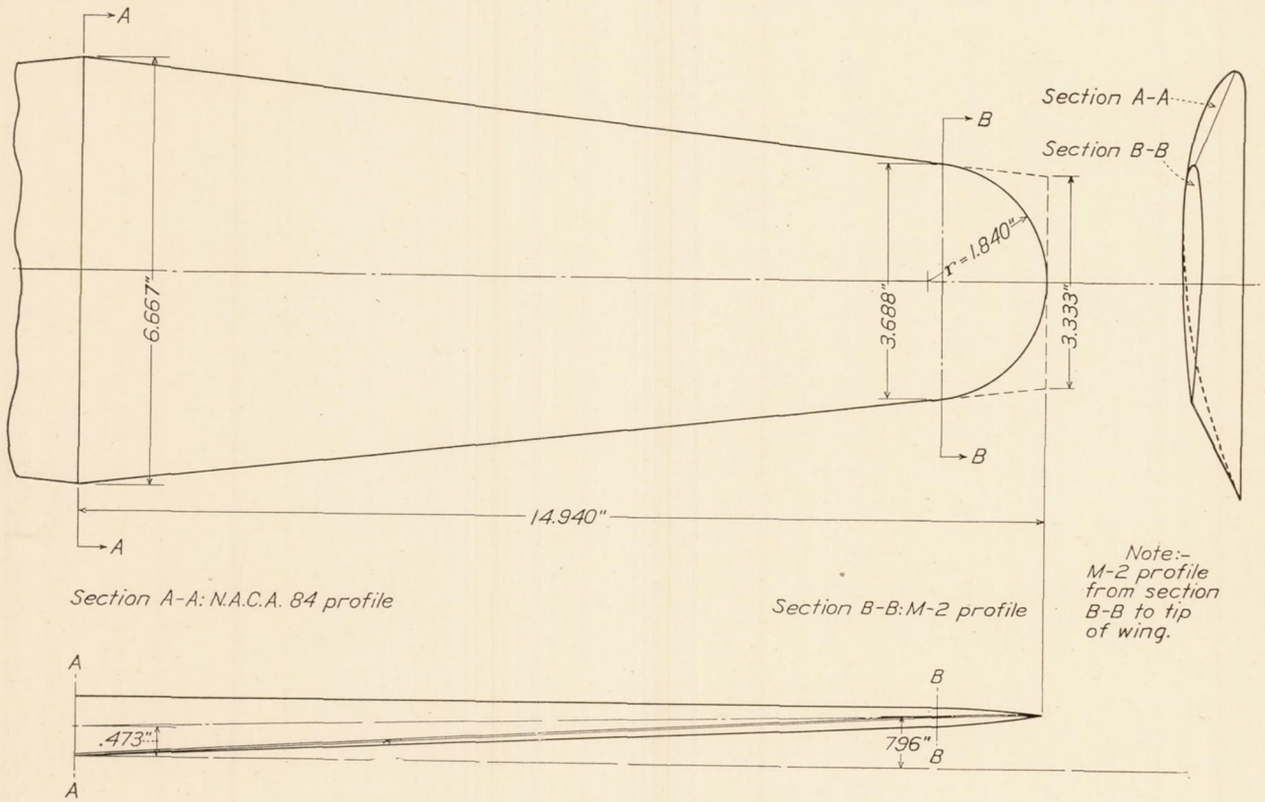

FIGURE 4.—Monoplane wing model—N. A. C. A. 86-M

The rates of stable autorotation were not corrected for the friction of the ball bearings, but this error is probably not greater than -2 per cent.

RESULTS

The results are presented as absolute coefficients in both tabular and graphical form. Tables IV to VII, inclusive, list the results of the stable-autorotation tests for the four wing models at various angles of attack and yaw, and Tables VIII to XXI give the results of the rolling-moment tests. Figures 9 to 35 give the results in the form of curves.

$\frac{pb}{2V}$ actually represents the ratio of the linear tip speed of the wing in the plane of rotation to the wind velocity. This coefficient, which is nondimensional, may be defined as follows:

$$\frac{pb}{2V}=\tan \varphi_t$$

where

p = angular velocity (radians per second).
b = span of wing.
V = wind velocity.
φ_t = difference between angle of attack at the wing tip and that at mid span.

The rolling-moment coefficient, C_λ, was used as applying to a wing when in rotation, rather than the usual rolling-moment coefficient which is ordinarily used for a *nonrotating* wing. It should be noted, however, that C_λ is identical with C_L at zero rate of rotation. The former may be defined as:

$$C_\lambda=\frac{\lambda}{qbS}$$

where

C_λ = absolute coefficient of rolling moment,
λ = measured rolling moment about dynamometer axis,
S = area of the wing,
b = span of the wing,
q = dynamic pressure,

all in a consistent system of units.

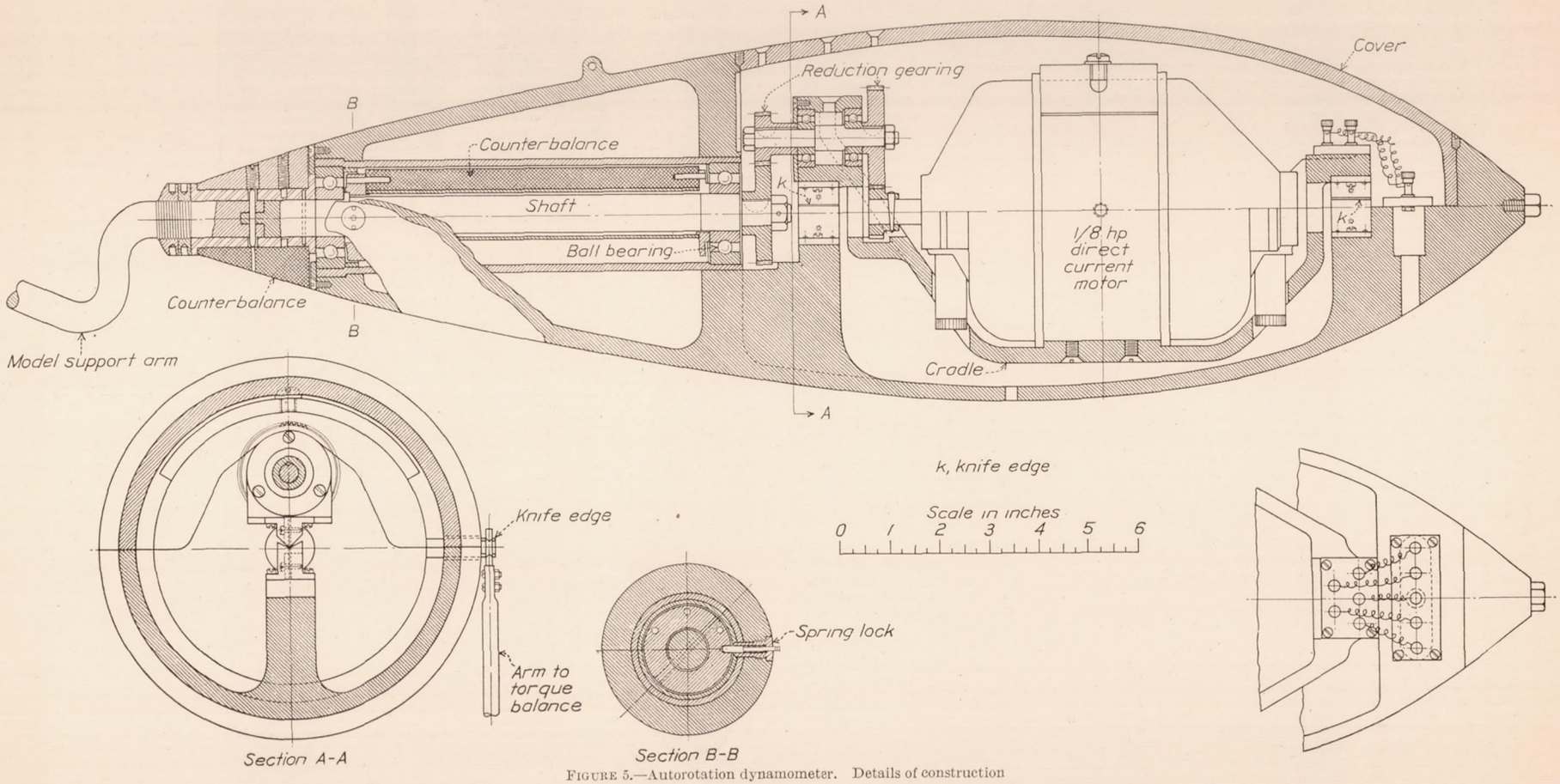

FIGURE 5.—Autorotation dynamometer. Details of construction

DISCUSSION

A general analysis of the rolling moments due to rolling and yaw will first be made, using as a basis the N. A. C. A. 84 monoplane wing, for which not only autorotation but also pressure-distribution data are available. A comparison will then be made of the autorotation test results on all four wing models.

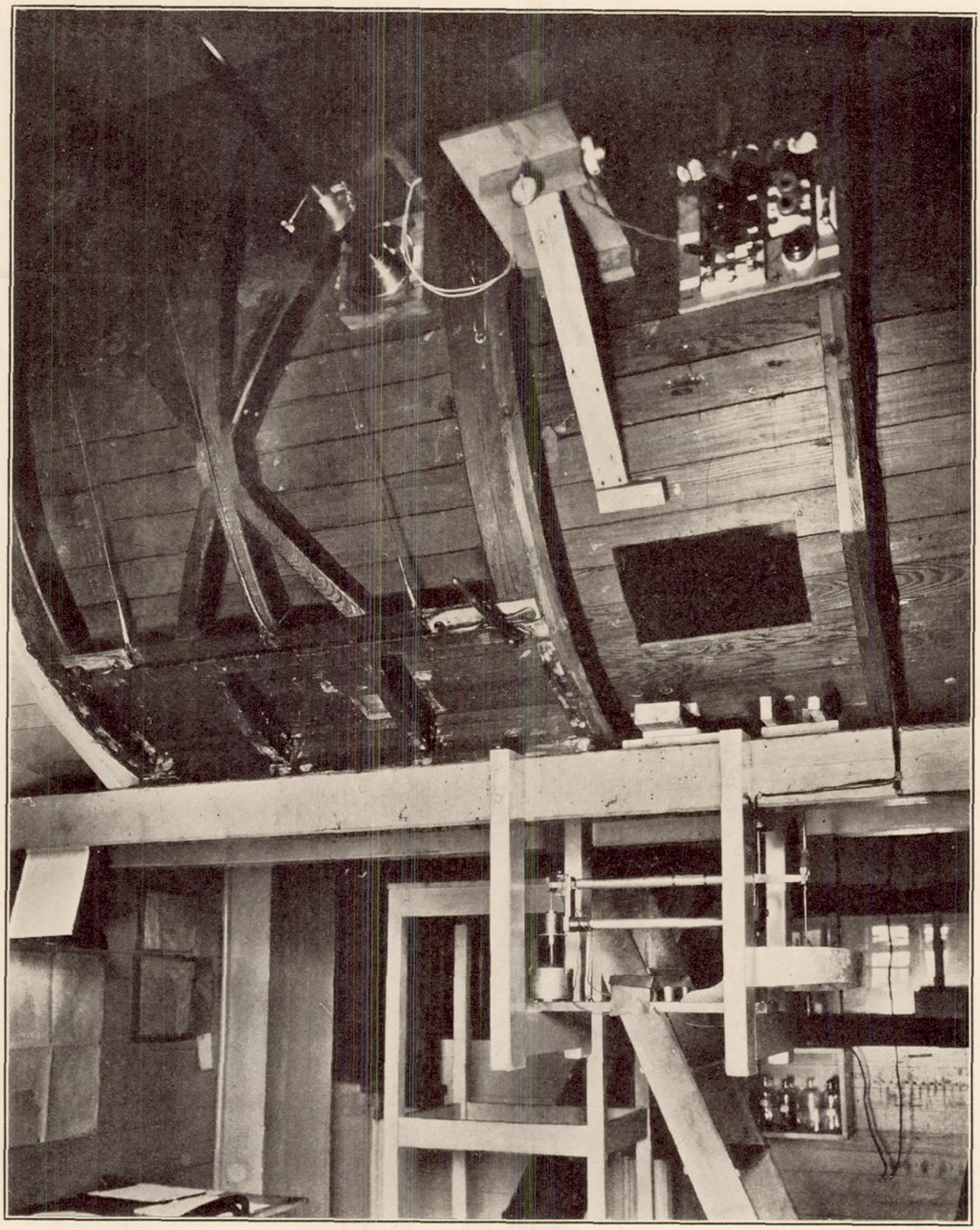

FIGURE 6.—Torque balance installation

In the tests the axis of yaw was in a plane parallel to the wind direction and normal to the plane of the wing chords. This is not the conventional axis of yaw. However, the design of the dynamometer apparatus as used in these tests permitted yawing the wing only about this axis. It is also to be noted that the angle-of-attack axis was always normal to the wind direction in these tests. (See Table XXVII for standard equivalents.)

The characteristic curves of rolling-moment coefficient, C_λ, due to rolling (yaw $=0°$) versus $\frac{pb}{2V}$ for the N. A. C. A. 84 wing, as obtained on the dynamometer, are shown in Figure 9. The dashed portions of the curves represent estimated fairings where it was impossible to obtain test data, owing to instability of the wing and dynamometer combination. Small moments occurring at $\frac{pb}{2V}=0$ are due to asym-

metry of the models or of the air flow in the tunnel. Rolling moments for rotations in both directions are plotted. Clockwise is positive and counter clockwise is negative direction of rotation.

The significance of these curves will be described briefly. Moments plotted in the first and third quadrants are those which aid, and in the second and fourth those which oppose, rotation. The change in the shape of the curves between $\alpha=12°$ and $\alpha=18°$ is noteworthy and characteristic of angles in the vicinity of maximum lift.

Let us now consider the curve for $\alpha=16°$. If the wing is started rotating in the positive direction, a moment opposing the rotation is set up. This moment reaches a maximum at $\frac{pb}{2V}=0.12$, thereupon decreasing until it becomes zero at $\frac{pb}{2V}=0.19$. At this point the wing would rotate of its own accord if it were not for the unstable condition represented by the positive slope of the curve as it crosses the axis. In other words, if the wing were left to itself at this point, a small disturbance tending to reduce the angular velocity would result in setting up a retarding moment, and the wing would come to rest. If, on the other hand, the disturbance increased the angular velocity, a moment aiding the rotation would be built up, reaching a maximum at about $\frac{pb}{2V}=0.26$, and then decreasing to zero at $\frac{pb}{2V}=0.35$. Here the rolling moment is once more zero, and since the slope of the curve is now negative, or opposite to the slope at the first intersection with the axis, a stable condition results, so that the wing will now rotate continuously, regardless of small momentary disturbances. The first condition may be termed "unstable autorotation" and the second "stable autorotation."

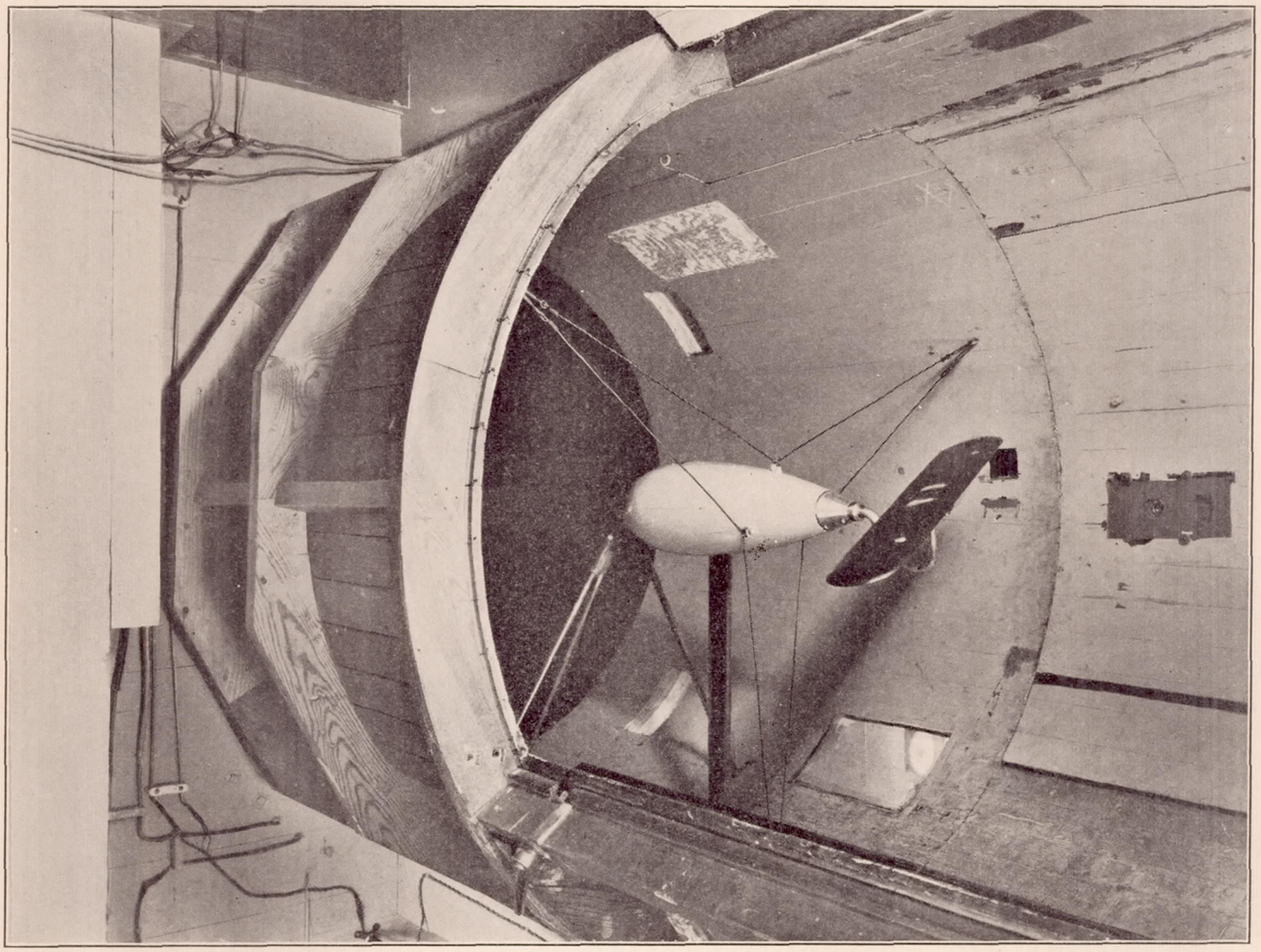

FIGURE 7.—Wing and dynamometer set-up in wind tunnel

It is evident that if the model were mounted so as to rotate freely when disturbed from rest, its rotation would build up until the stable-autorotation point for the particular angle of attack was reached. (This point will be attained, however, only if the disturbance is of sufficient magnitude to carry the rotation beyond any unstable-autorotation points first encountered.) The results of such a stable-autorotation test on the N. A. C. A. 84 wing are given in Figure 10, in which

$\frac{pb}{2V}$ is plotted versus angle of attack, α. To obtain the data for this curve, the dynamometer gearing was thrown out of mesh so that the model could turn freely with the shaft, which is mounted on ball bearings, as explained previously. The reversal of the direction of the curve near $\alpha = 15°$ can be explained by reference again to the curve for $\alpha = 16°$ in Figure 9. Here it will be seen that the model must be forced to rotate up to the point of unstable autorotation, beyond which it will rotate of its own accord. This point, together with the stable-autorotation points, as obtained from the moment curves of Figure 9, is plotted in Figure 10. The slight differences between these points and the curve are due to the small tare moments produced by friction in the ball bearings and the windage of the arm supporting the model. The point on the axis at $\alpha = 21°$ was obtained by decreasing the angle until the wing would no longer rotate when disturbed slightly from rest.

Let us now consider the rolling moment due to yaw. The total rolling moments due to both rolling and yaw for the N. A. C. A. 84 wing (yaw = 10°) are plotted in Figure 11, which has the same ordinates as the figure for zero yaw (Fig. 9). The convention adopted in this figure is that for positive values of $\frac{pb}{2V}$ the rolling moments due to the yaw and the roll are in the same sense, and for negative values they oppose each other. For the tests in yaw the wing was given only positive yaw, i. e., the right wing tip was back, but rotations were taken in both positive and negative directions.

The general effect of yaw is to raise the curves as a group. It will also be seen that large moments now exist at $\frac{pb}{2V} = 0$. The changes in rolling moment due to yaw with changes in $\frac{pb}{2V}$ are of interest, and these are shown in Figure 12 for five selected angles of attack. These curves were obtained merely by taking the differences between the corresponding curves of rolling moment due to rolling (fig. 9) and rolling moment due to rolling and yaw (fig. 11). They indicate that the maximum moments due to yaw occur at the angles of attack of stable autorotation and in the vicinity of $\frac{pb}{2V} = 0$. The variation with $\frac{pb}{2V}$ is much greater

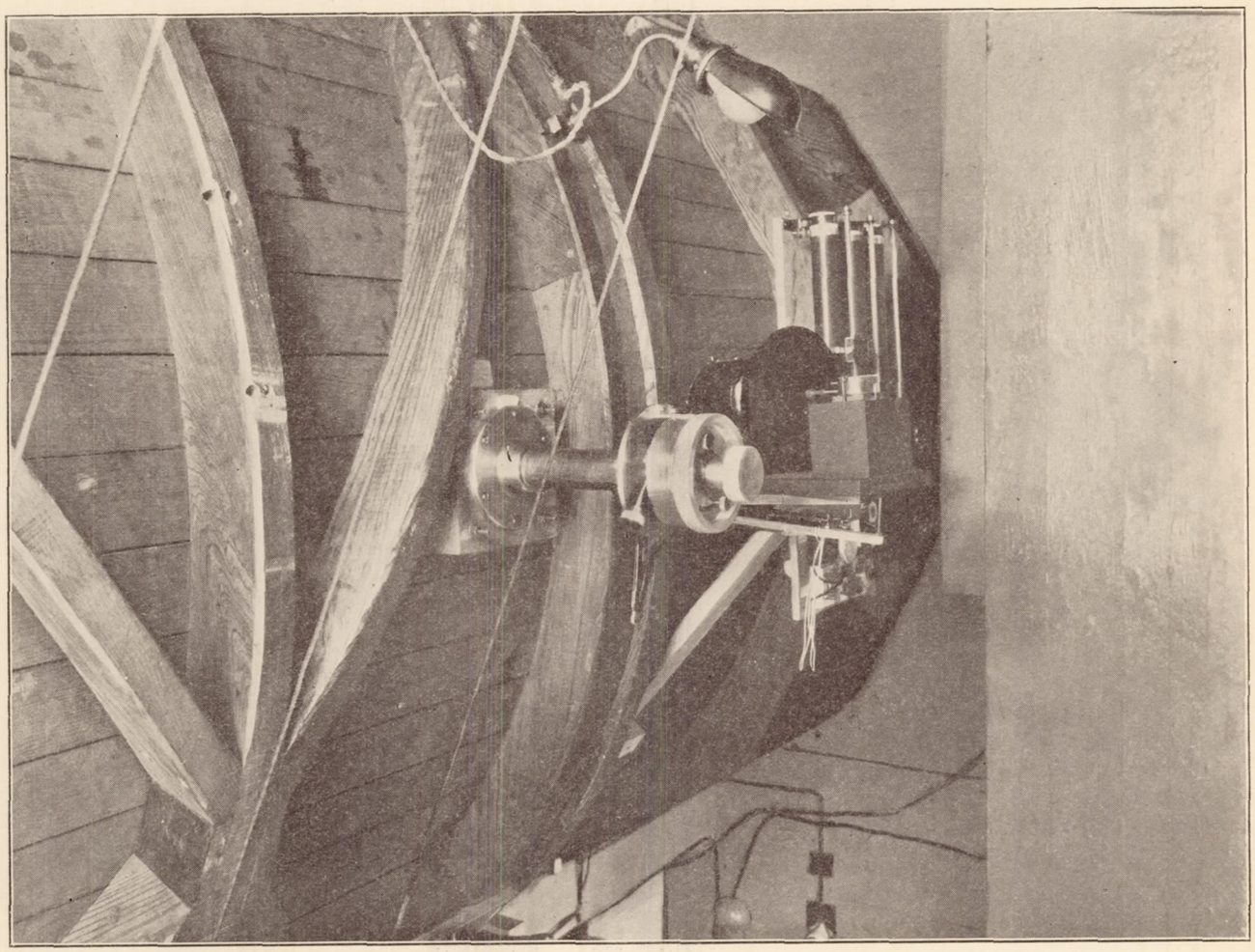

FIGURE 8.—Mechanism inserted for changing angle of attack

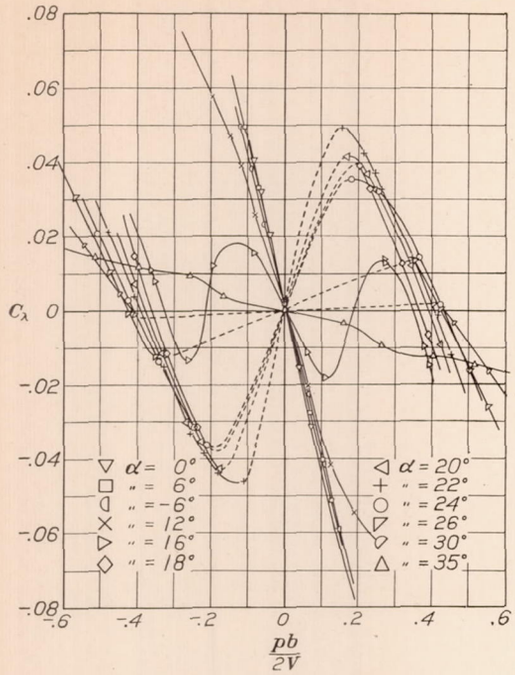

FIGURE 9.—Rolling moment coefficient vs. $\frac{pb}{2V}$ for N. A. C. A. 84 monoplane wing model. Yaw=0°

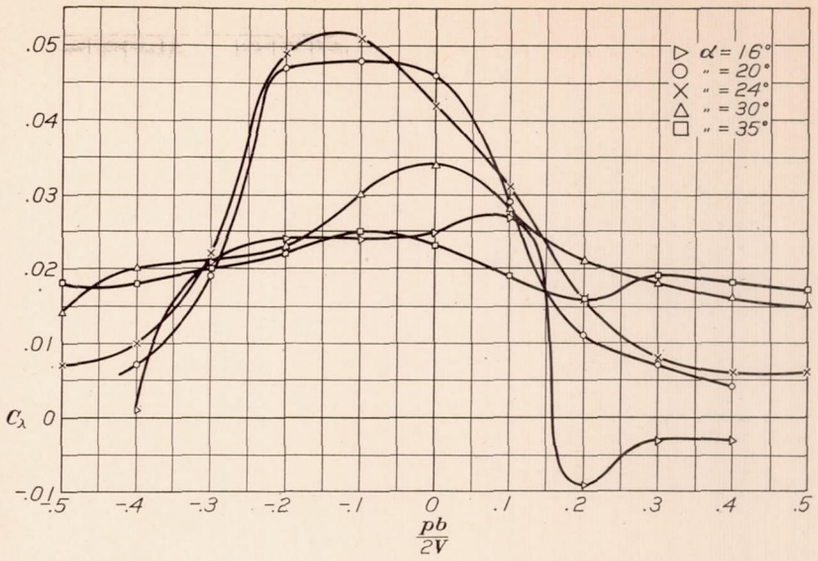

FIGURE 12.—Rolling moment due to yaw vs. $\frac{pb}{2V}$ for N. A. C. A. 84 monoplane wing model. Yaw=10°

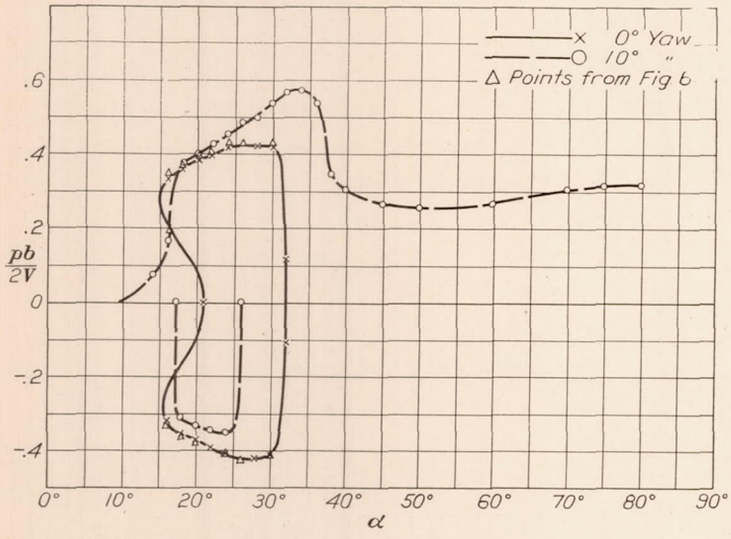

FIGURE 10.—$\frac{pb}{2V}$ vs. angle of attack for N. A. C. A. 84 monoplane wing model. Yaw=0°, 10°

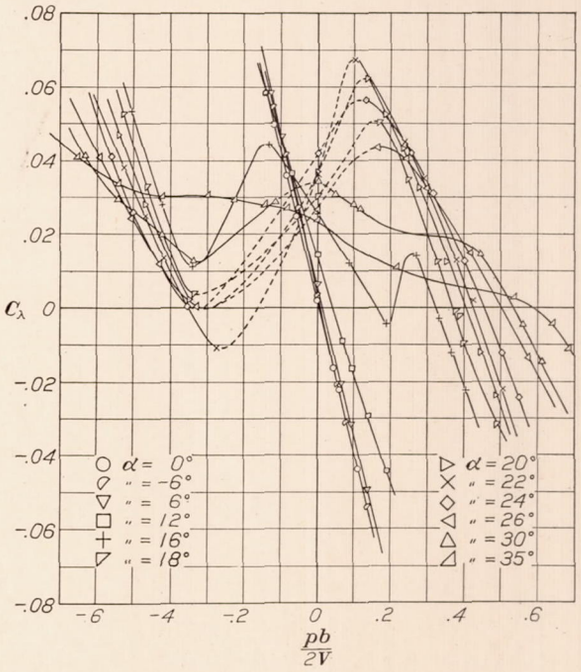

FIGURE 11.—Rolling moment coefficient vs. $\frac{pb}{2V}$ for N. A. C. A. 84 monoplane wing model. Yaw=10°

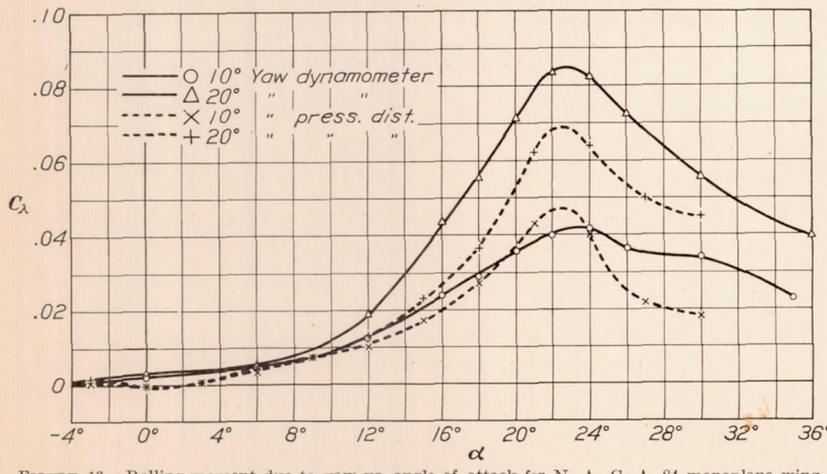

FIGURE 13.—Rolling moment due to yaw vs. angle of attack for N. A. C. A. 84 monoplane wing model. Yaw=10°, 20°

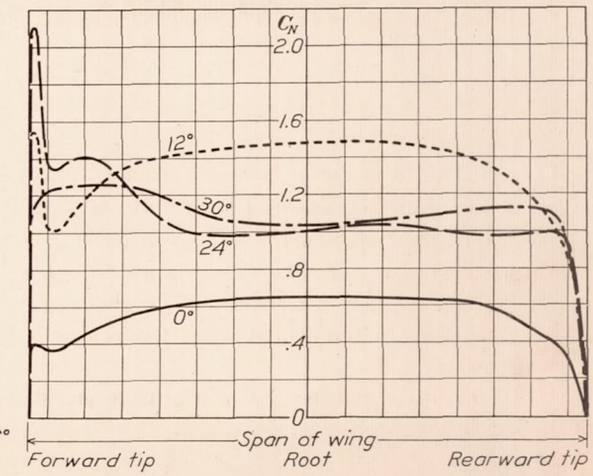

FIGURE 14.—Span load distribution for N. A. C. A. 84 monoplane wing model. Yaw=10°

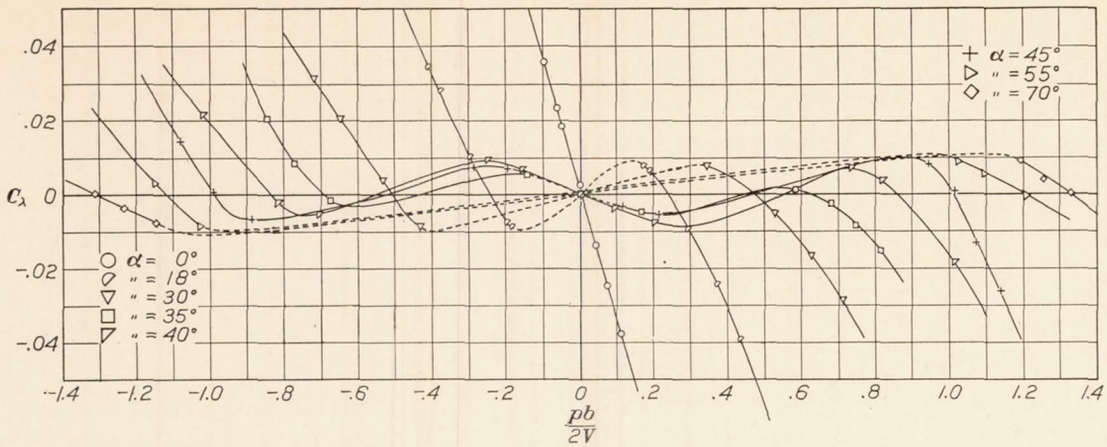

FIGURE 15.—Rolling moment coefficient vs. $\frac{pb}{2V}$ for Clark Y biplane wing model. Yaw=0°

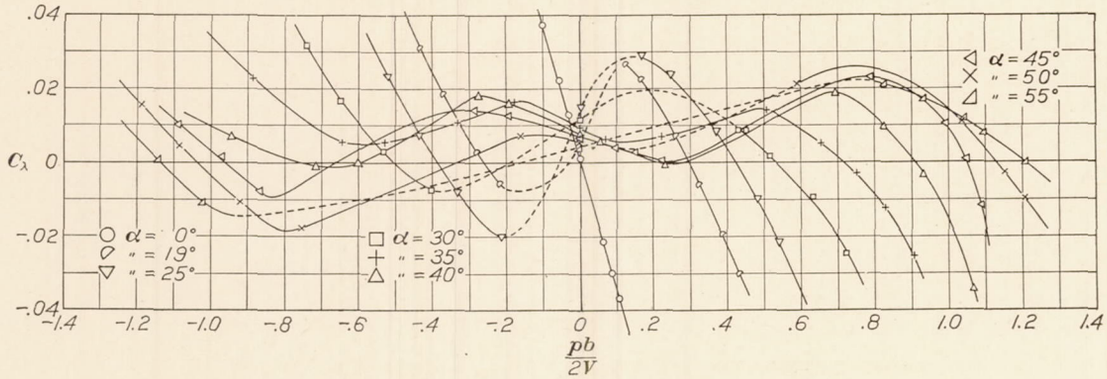

FIGURE 16.—Rolling moment coefficient vs. $\frac{pb}{2V}$ for Clark Y biplane wing model. Yaw=5°

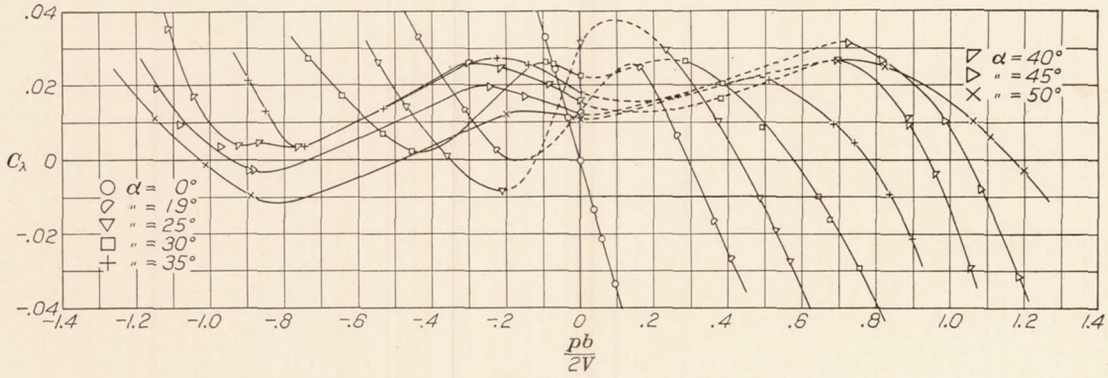

FIGURE 17.—Rolling moment coefficient vs. $\frac{pb}{2V}$ for Clark Y biplane wing model. Yaw=10°

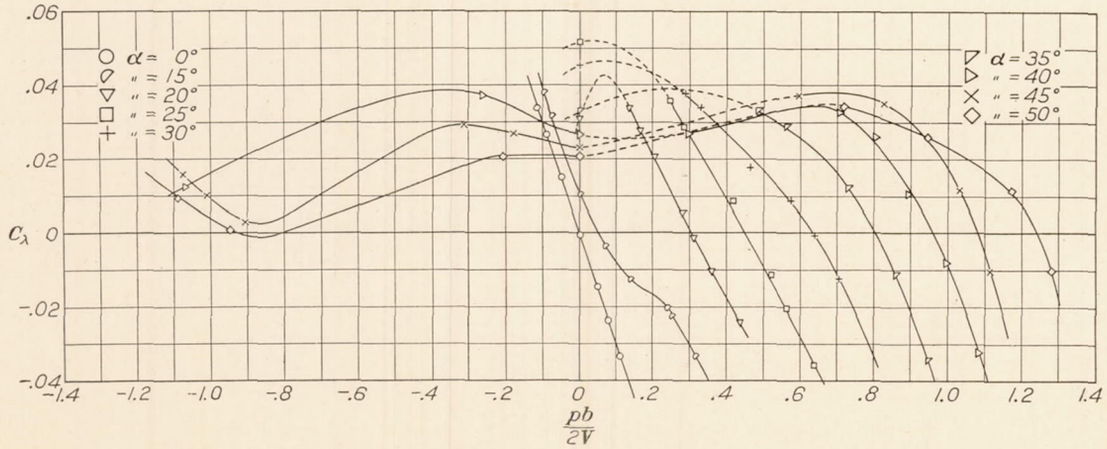

FIGURE 18.—Rolling moment coefficient vs. $\frac{pb}{2V}$ for Clark Y biplane wing model. Yaw=20°

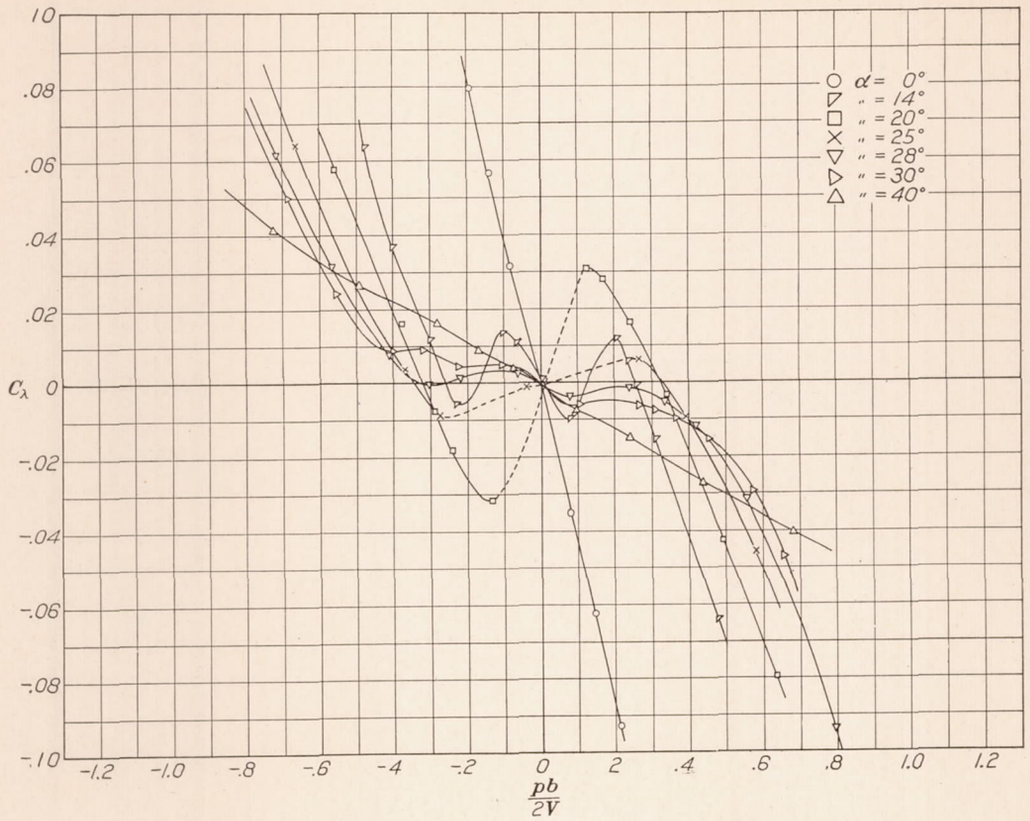

FIGURE 19.—Rolling moment coefficient vs. $\frac{pb}{2V}$ for Clark Y monoplane wing model. Yaw=0°

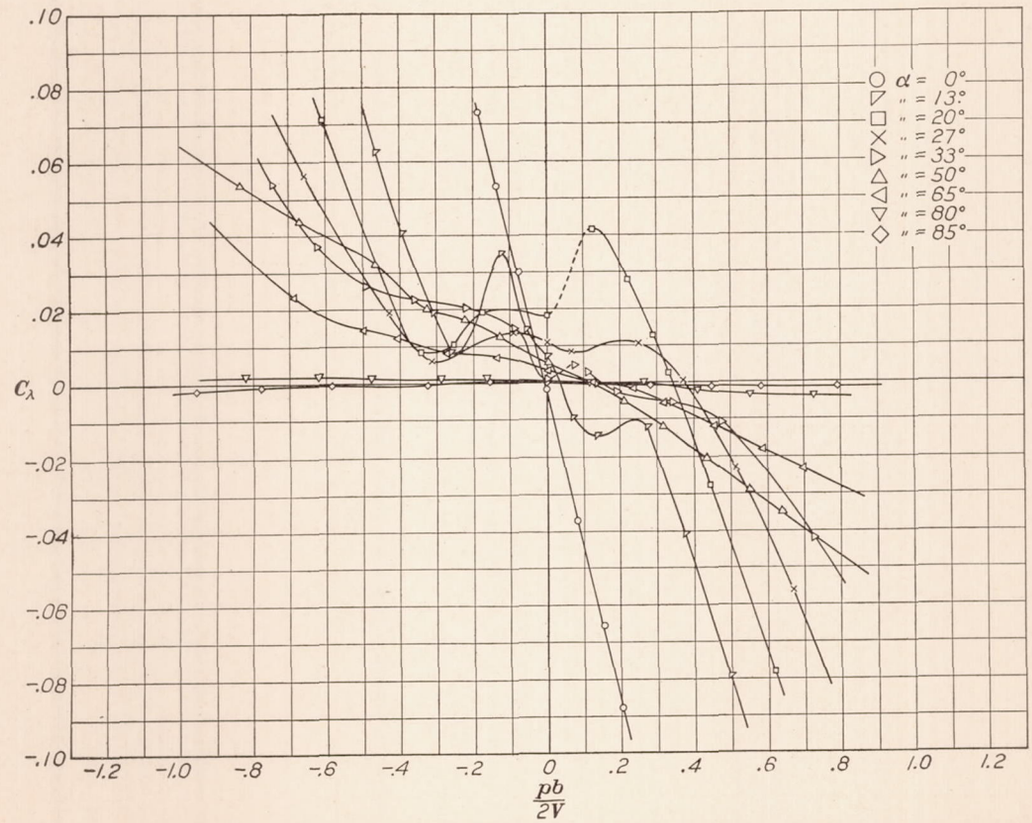

FIGURE 20.—Rolling moment coefficient vs. $\frac{pb}{2V}$ for Clark Y monoplane wing model. Yaw=5°

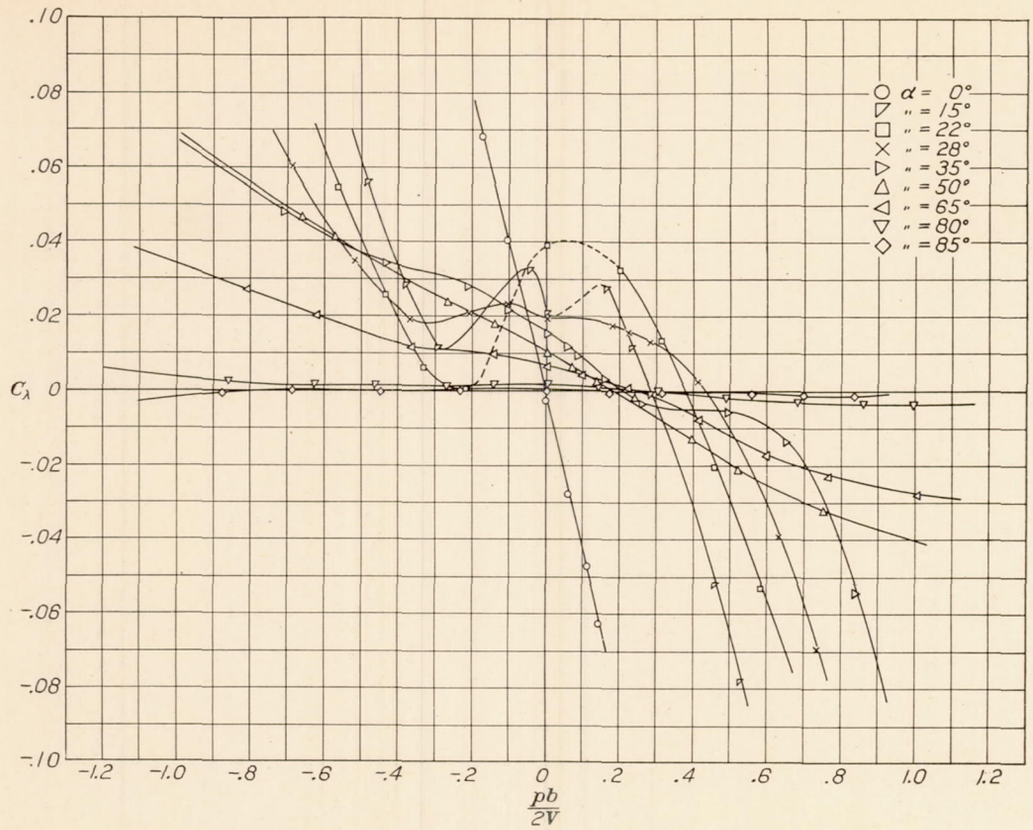

FIGURE 21.—Rolling moment coefficient vs. $\frac{pb}{2V}$ for Clark Y monoplane wing model. Yaw=10°

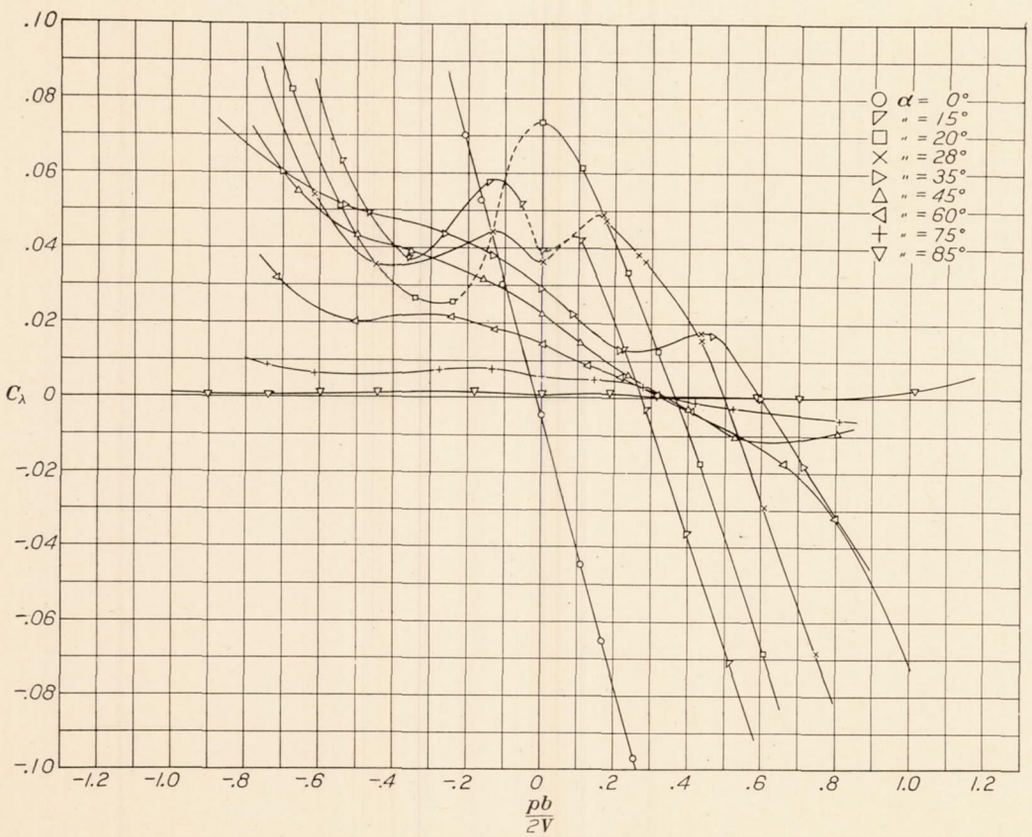

FIGURE 22.—Rolling moment coefficient vs. $\frac{p\,b}{2V}$ for Clark Y monoplane wing model. Yaw=20°

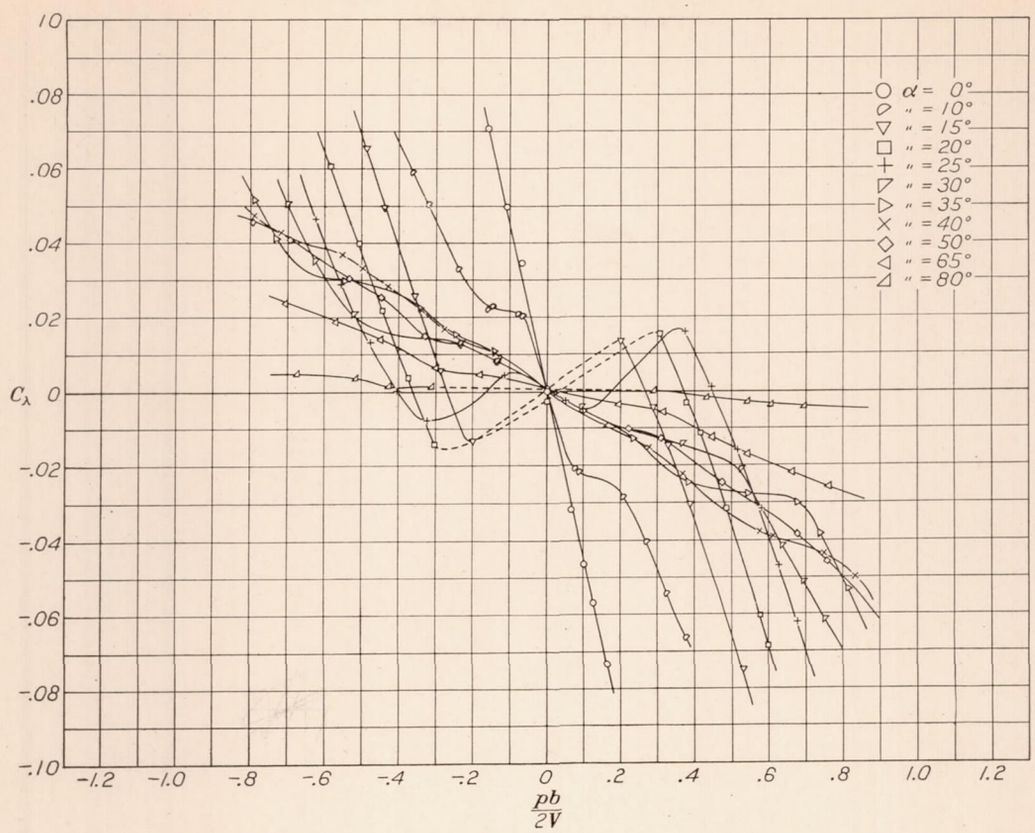

FIGURE 23.—Rolling moment coefficient vs. $\frac{pb}{2V}$ for N. A. C. A. 86–M monoplane wing model. Yaw=0°

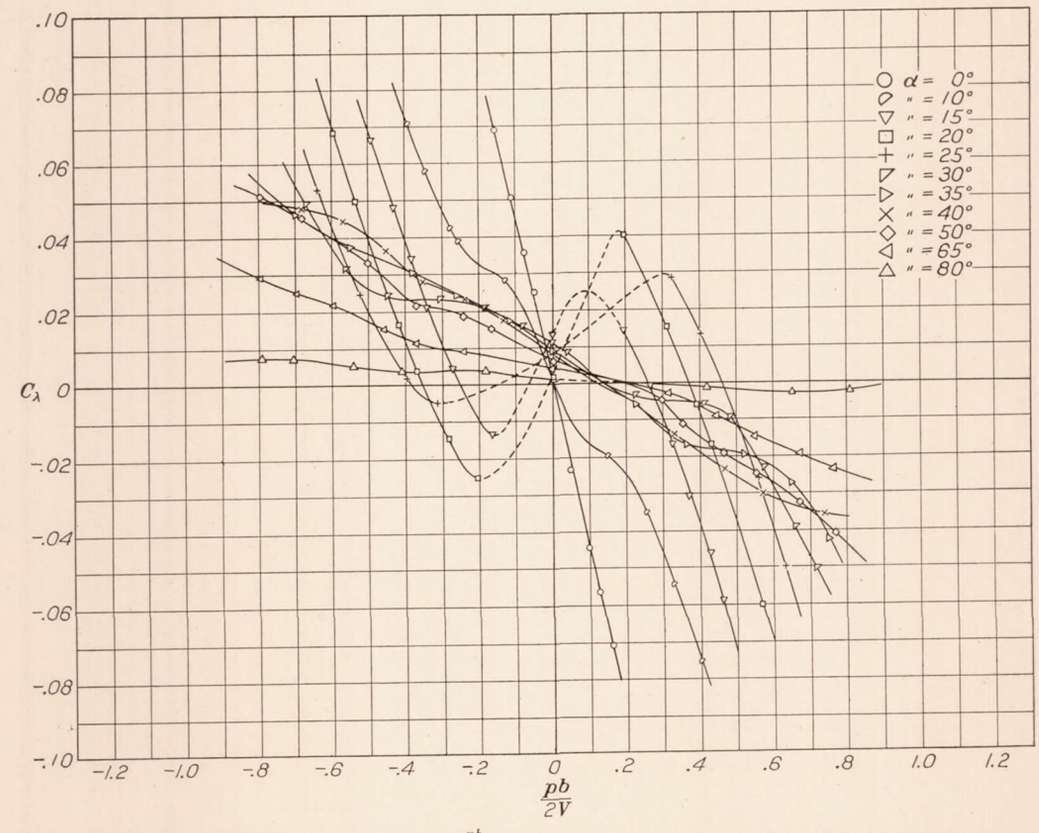

FIGURE 24.—Rolling moment coefficient vs. $\frac{pb}{2V}$ for N. A. C. A. 86–M monoplane wing model. Yaw=5°

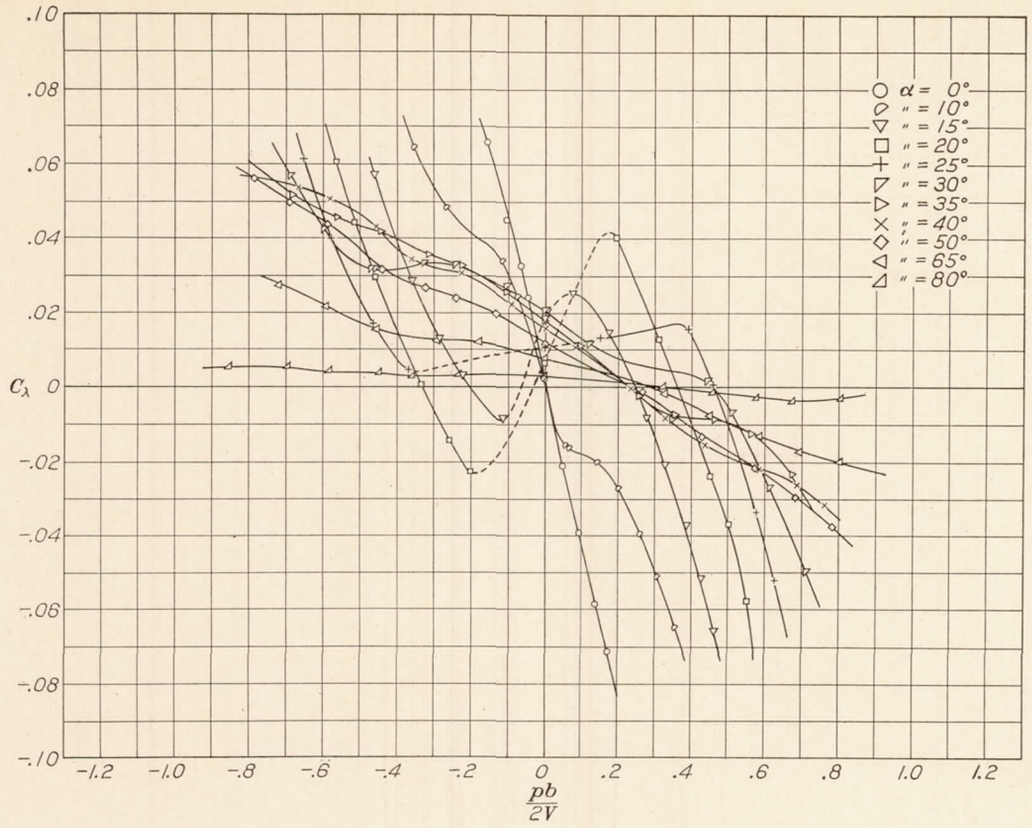

FIGURE 25.—Rolling moment coefficient vs. $\frac{pb}{2V}$ for N. A. C. A. 86-M monoplane wing model. Yaw=10°

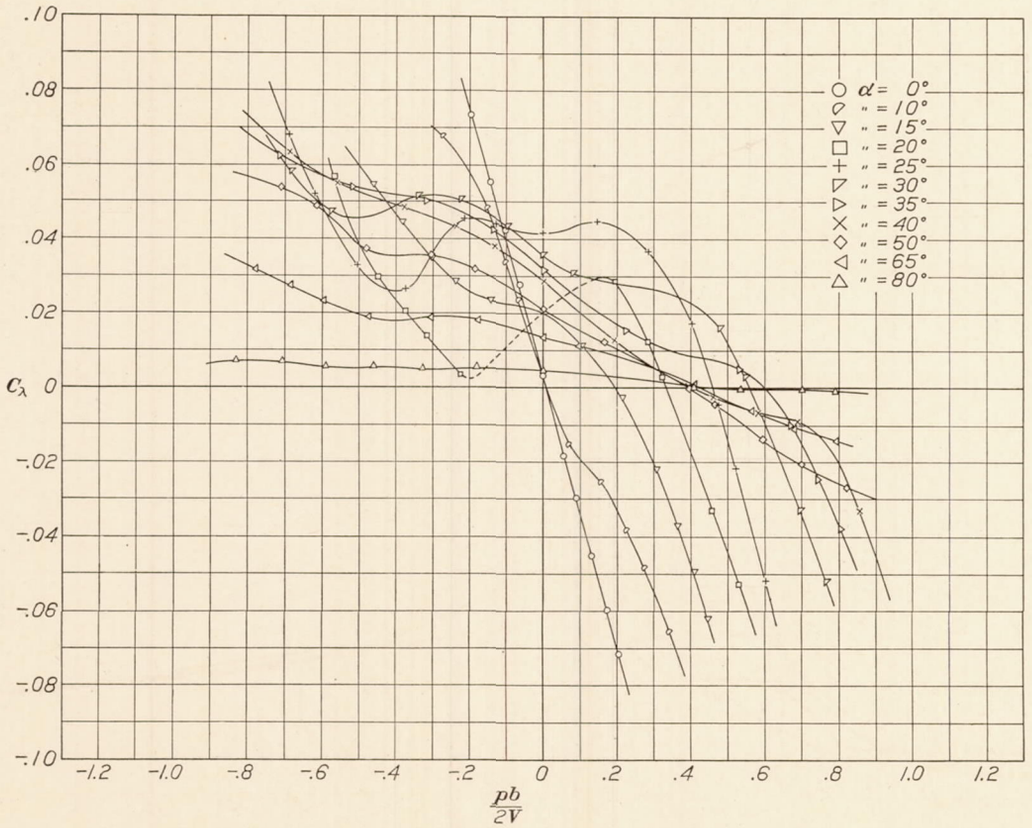

FIGURE 26.—Rolling moment coefficient vs. $\frac{pb}{2V}$ for N. A. C. A. 86-M monoplane wing model. Yaw=20°

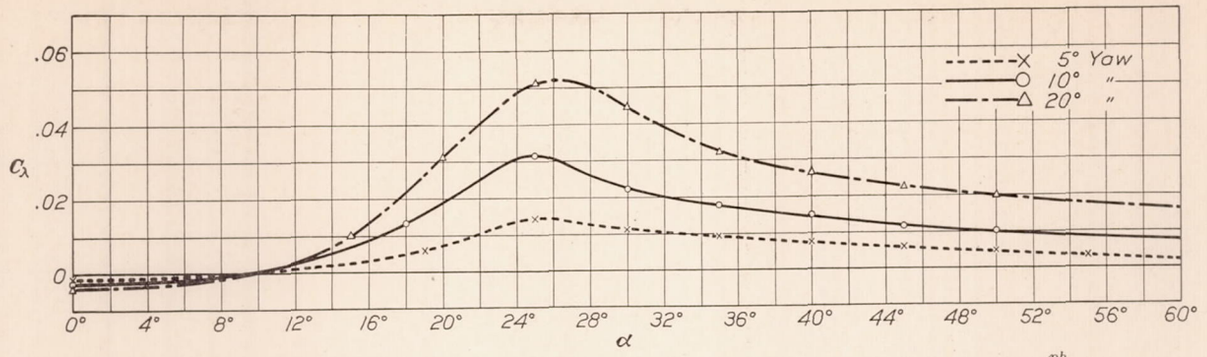

FIGURE 27.—Rolling moment due to yaw vs. angle of attack for Clark Y biplane wing model. Yaw=5°, 10°, 20°. $\frac{pb}{2V}=0$

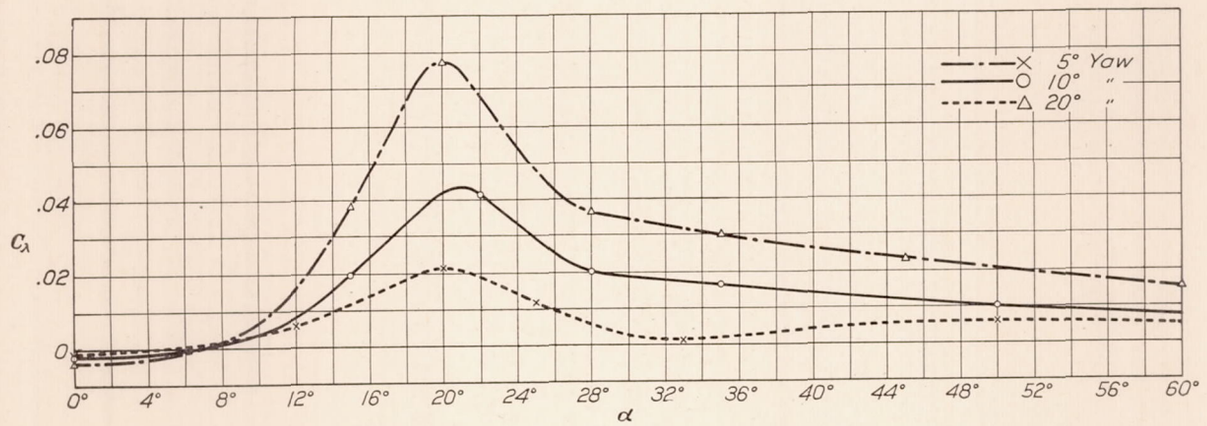

FIGURE 28.—Rolling moment due to yaw vs. angle of attack for Clark Y monoplane wing model. Yaw=5°, 10°, 20°. $\frac{pb}{2V}=0$

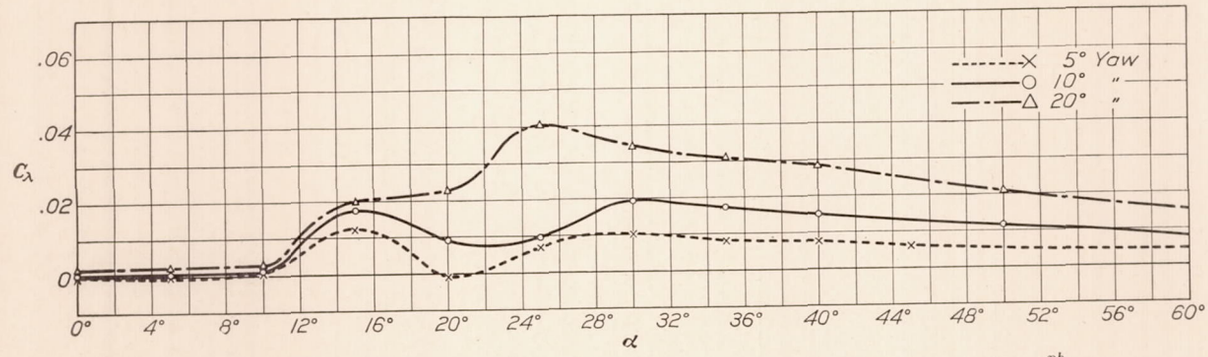

FIGURE 29.—Rolling moment due to yaw vs. angle of attack for N. A. C. A. 86-M monoplane. Yaw=5°, 10°, 20°. $\frac{pb}{2V}=0$

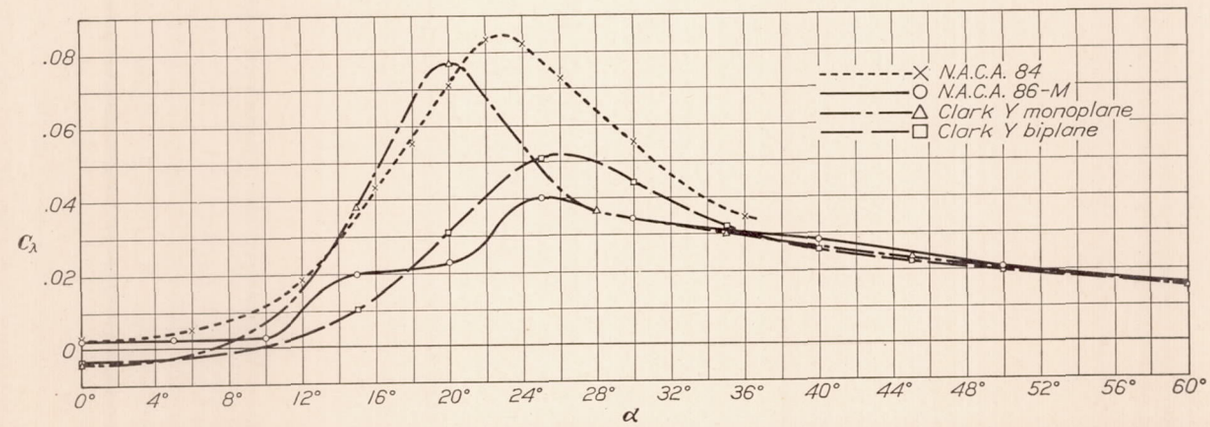

FIGURE 30.—Rolling moment due to yaw vs. angle of attack for four wing models. Yaw=20°. $\frac{pb}{2V}=0$

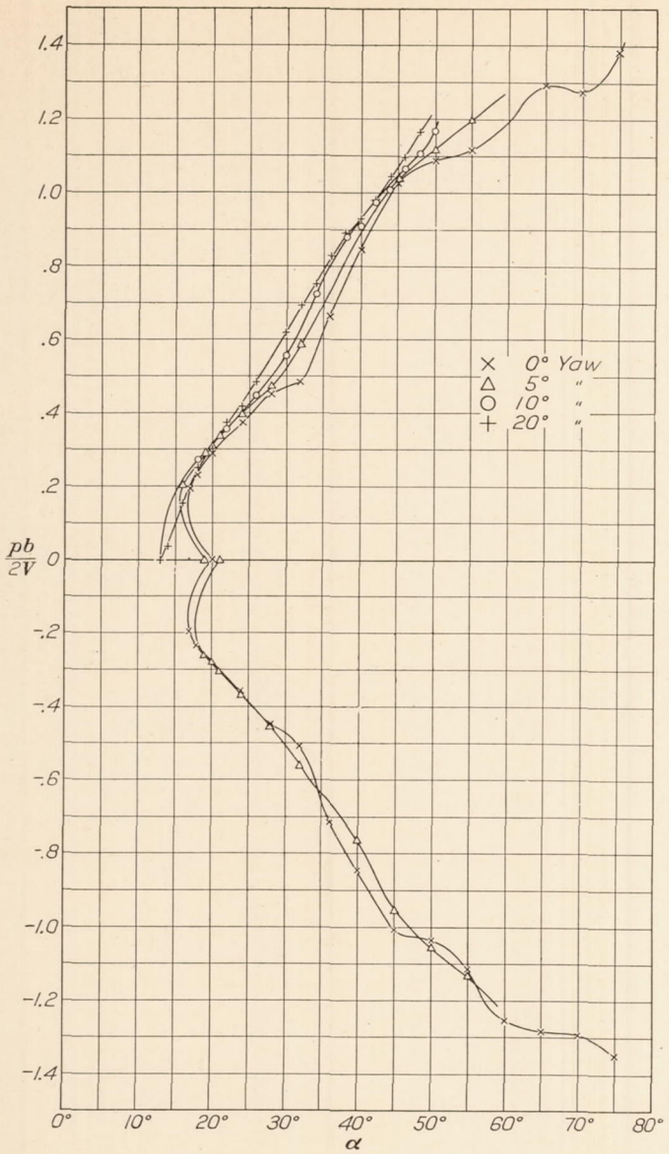

FIGURE 31.—$\frac{pb}{2V}$ vs. angle of attack for Clark Y biplane wing model. Yaw=0°, 5°, 10°, 20°

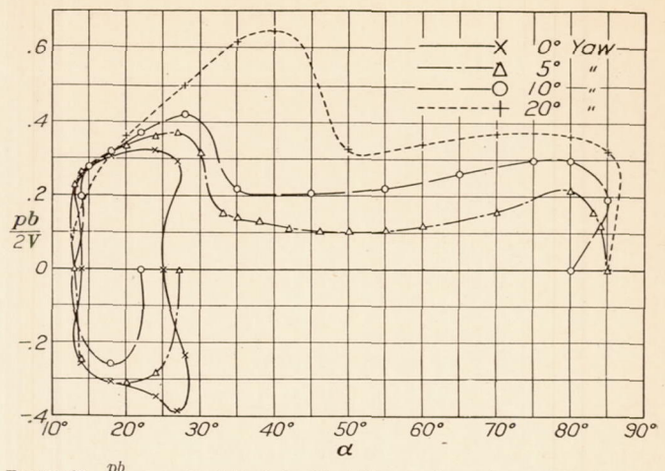

FIGURE 32.—$\frac{pb}{2V}$ vs. angle of attack for Clark Y monoplane wing model. Yaw=0° 5°, 10°, 20°

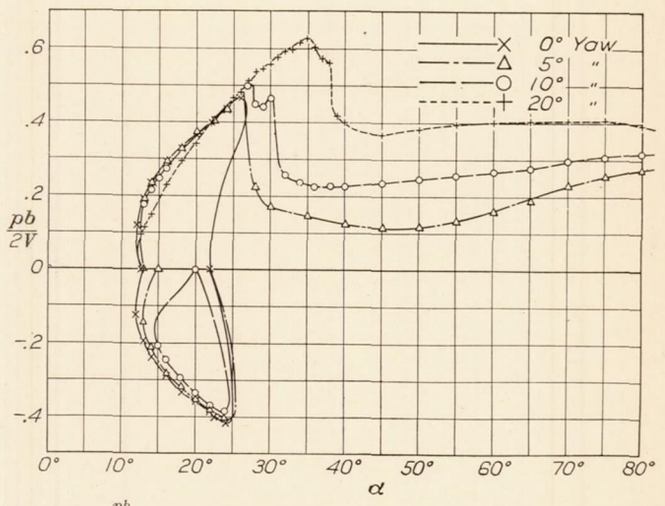

FIGURE 33.—$\frac{pb}{2V}$ vs. angle of attack for N. A. C. A. 86-M monoplane wing model. Yaw=0°, 5°, 10°, 20°

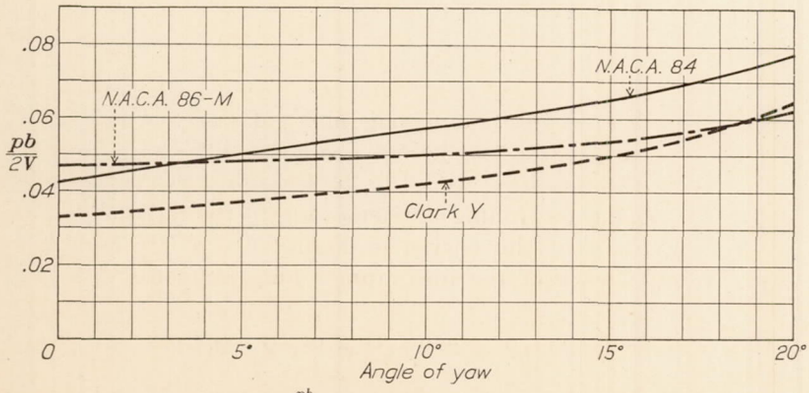

FIGURE 35.—Maximum $\frac{pb}{2V}$ vs. angle of yaw for three monoplane wing models

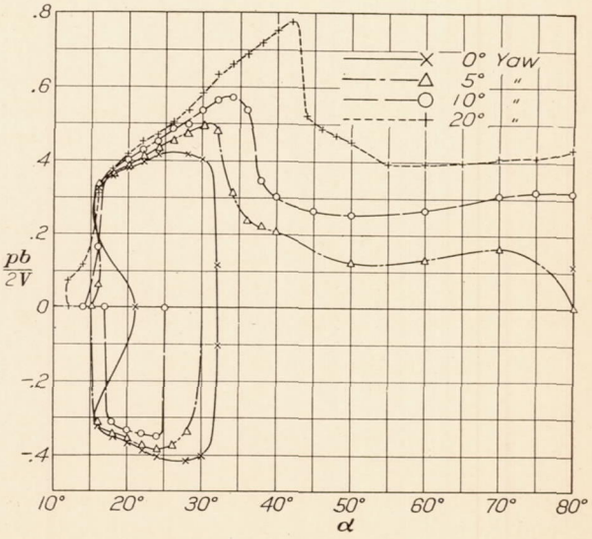

FIGURE 34.—$\frac{pb}{2V}$ vs. angle of attack for N. A. C. A. 84 monoplane wing model. Yaw=0°, 5°, 10°, 20°

between $\alpha=16°$ and $\alpha=30°$ than above the latter angle. It is of importance to note that positive moments for positive values of $\frac{pb}{2V}$ aid rotation, while positive moments for negative values of $\frac{pb}{2V}$ oppose it.

The curves of stable autorotation for 10° yaw for rotations in both directions are included in Figure 10. The marked differences in values of $\frac{pb}{2V}$ and in ranges agree with similar tests of this type described in References 7 and 8, mentioned previously. For positive values of $\frac{pb}{2V}$, rate and range of autorotation is considerably increased, while for negative values it is reduced.

A knowledge of the manner in which the span load distribution changes to produce a rolling moment when a wing is yawed may be expected to be of value in determining the reason for the existence of this peculiar moment at large angles of attack. A limited amount of such information is available for the N. A. C. A. 84 monoplane wing as the result of recent pressure-distribution tests. In certain of these tests the half-span wing model used was given an angle of sweep back and also sweep forward. The pressure-distribution results were analyzed on the basis of yaw by considering that yaw is equivalent to sweep forward on one half of the span and sweep back on the other half. The full-span rolling moments due to 10° and 20° yaw obtained in this manner from the half-span wing results are plotted in Figure 13, together with the moments obtained on the full-span wing mounted on the dynamometer. While the agreement is only fair, the trend is the same in each case and furnishes a justification for using the sweep-back and sweep-forward results for the purpose of this analysis.

The span-load distribution, as thus determined, is plotted in Figure 11 for a few selected angles. The cause of the rolling moment is at once apparent, for it is evident that as the angle of attack increases the loads increase on the forward wing, particularly at the tip, while the reverse is true for the rearward wing. This has also been found to be the case as a result of pressure-distribution tests made on a full-span wing model at various angles of yaw. (Reference 5.)

Let us now turn to a consideration of the results of tests on the other three wing systems: namely, the Clark Y unstaggered biplane, the Clark Y monoplane, and the N. A. C. A. 86–M monoplane. The characteristic curves of rolling-moment coefficient, C_λ, versus $\frac{pb}{2V}$ are given for yaw $=0°$, 5°, 10°, and 20° in Figures 15 to 26.

The values of C_λ at $\frac{pb}{2V}=0$ are plotted versus α for each wing at 5°, 10°, and 20° yaw in Figures 27, 28, and 29. The curves of this type for all four wing models at 20° yaw are assembled for comparison in Figure 30. It should be remembered, however, that the effect of the different-shaped tips is also included in this comparison, although the effects may be small. The maxima for all four curves occur between $\alpha=20°$ and 26°. The negative moments for the Clark Y models are probably due to the negative dihedral effect of the tips. (See figs. 1 and 2.) The Clark Y and N. A. C. A. 84 monoplane wings show similar results up to the vicinity of their maxima, beyond which the moments for the N. A. C. A. 84 wing are greater. The Clark Y biplane wing moments are much less than those for the Clark Y monoplane wing between $\alpha=6°$ and $\alpha=25°$, and greater beyond this angle up to $\alpha=36°$, above which they are almost identical for the limits of the tests. In fact, it appears that the values for all the wings may be expected to be practically the same above $\alpha=36°$. The value of the maximum moments decreases in the following order: N. A. C. A. 84 monoplane, Clark Y monoplane, Clark Y biplane, and N. A. C. A. 86–M monoplane. The peculiar additional bend in the N. A. C. A. 86–M curve at about $\alpha=14°$ should be noted.

The stable-autorotation characteristics of each wing at 0°, 5°, 10°, and 20° yaw are given in Figures 31 to 34. All of the monoplane-wing results are affected in the same general manner when the angle of yaw is increased, there being a general increase in both the rates and ranges of autorotation. The variation of the maximum values of $\frac{pb}{2V}$ with angle of yaw are plotted for the three monoplane wings in Figure 35. A yaw of 20° practically doubles the maximum value of $\frac{pb}{2V}$ at zero yaw for the N. A. C. A. 84 and Clark Y monoplanes, whereas for the N. A. C. A. 86–M wing the increase is only about one-third. The biplane stable-autorotation rates are not greatly changed by yaw, as may be seen in Figure 31.

In order that a wing have dynamic lateral stability, it is essential, among other things, that a righting (rolling) moment due to side slip (yaw) be accompanied by a damping moment due to roll. Below the stall the damping moments are usually ample for stability in comparison with the righting moments. In general above the stall, however, the damping moment changes sign and becomes an accelerating moment, and the righting moment due to side slip assumes large proportions. A possibility of improving this situation would be to seek for some means of reducing the rolling moments due to rolling and yaw. A study of the curves in Figures 9, 15, 19, and 23 indicates that the maximum rolling moments due to rolling can be reduced a considerable extent by using an unstaggered biplane wing or by tapering a monoplane wing in plan and thickness.

Several additional subjects for future investigation suggest themselves as a result of this work. One of importance is the further study of biplane wings to determine the effects of stagger and gap on the rolling moments due to rolling and to yaw. In the same connection an investigation of more highly tapered wings than are now in use would also appear to furnish some useful information regarding the monoplane characteristics.

CONCLUSIONS

1. At angles of attack above that of maximum lift the rolling moments on wings due to yaw (or side slip) from 5° to 20° are of the same order of magnitude as those due to rolling.

2. There is a wide variation in the magnitude of the rolling moment due to yaw angle with both angle of attack and rate of roll.

3. The rates and ranges of stable autorotation for the monoplane wings are considerably increased by yaw, whereas for an unstaggered biplane they are little affected.

4. The immediate cause of the rolling moment due to yaw angle is, apparently, the building up of large tip loads on the forward wing and the reduction of tip loads on the rearward wing.

LANGLEY MEMORIAL AERONAUTICAL LABORATORY,
NATIONAL ADVISORY COMMITTEE FOR AERONAUTICS,
LANGLEY FIELD, VA., *August 19, 1930.*

REFERENCES

1. Irving, H. B., and Batson, A. S.: The Effects of Stagger and Gap on the Aerodynamic Properties of Biplanes at Large Angles of Attack. B. A. R. C. Reports and Memoranda No. 1064, 1927.
2. Iriving, H. B., and Batson, A. S.: Experiments on a Model of a Bristol Fighter Aeroplane. Section 1, Force and Moment Measurements at Various Angles of Yaw. B. A. R. C. Reports and Memoranda No. 932, 1924.
3. Irving, H. B., and Batson, A. S.: Forces and Moments (Including Those Due to Controls) on a Model Fairey "N4" Flying Boat *Atlanta* at Various Angles of Yaw. B. A. R. C. Reports and Memoranda No. 933, 1924.
4. Batson, A. S.: Experiments on a Model of a Fokker (F. VII) Monoplane Wing. Part I, Rolling and Yawing Moments Due to Rolling and Ailerons. B. A. R. C. Reports and Memoranda No. 1059, 1926.
5. Williams, D. H.: Pressure Distribution Over a Yawed Aerofoil. B. A. R. C. Reports and Memoranda No. 1203, 1928.
6. Jones, Melville B., and Maitland, C. E.: Instrumental Records of the Lateral Motions of a Stalled Bristol Fighter Aeroplane. B. A. R. C. Reports and Memoranda No. 1181, 1928.
7. Hardy, J. K.: Full-Scale Control Tests on Fokker F. VII 3M Monoplane. B. A. R. C. Reports and Memoranda No. 1228, 1928.
8. Ober, Shatswell: Some Experiments on Autorotation of an Airfoil. N. A. C. A. Technical Note No. 319, 1929.
9. La Presle, A.: Girouette Aerodynamique et Stabilité de Forme des Planeurs. Services Technique de L'Aeronautique. Bulletin Technique No. 66, 1930.
10. Bradfield, J. B., and Simmonds, O. E.: Rolling and Yawing Moments Due to Roll of Model Avro Wings with Standard and Interplane Ailerons and Rudder Moments for Standard and Special Large Rudder. B. A. R. C. Reports and Memoranda No. 848, 1922.
11. Hoot, H. I.: The Effect of Airfoil Thickness and Plan Form on Lateral Control. N. A. C. A. Technical Report No. 169, 1923.
12. Reid, Elliott G.: Standardization Tests of N. A. C. A. No. 1 Wind Tunnel. N. A. C. A. Technical Report No. 195, 1924.

TABLE I.—ORDINATES, CLARK Y WING

[Monoplane and biplane]

Station (% c from L. E.)	Upper (% c)	Lower (% c)	Station (% c from L. E.)	Upper (% c)	Lower (% c)
0	3.50	3.50	40.00	11.40	0
1.25	5.45	1.93	50.00	10.52	0
2.50	6.50	1.47	60.00	9.15	0
5.00	7.90	.93	65.00	8.30	0
7.50	8.85	.63	70.00	7.35	0
10.00	9.60	.42	80.00	5.22	0
15.00	10.69	.15	90.00	2.82	0
20.00	11.36	.03	95.00	1.49	0
30.00	11.70	0	100.00	.12	0

TABLE II.—ORDINATES, N. A. C. A. 84 WING

Station (% c from L. E.)	Upper (% c)	Lower (% c)	Station (% c from L. E.)	Upper (% c)	Lower (% c)
0	2.50	2.50	30.00	14.00	0
.50	3.90	1.55	35.00	14.18	0
1.25	4.85	.95	40.00	14.11	0
2.50	6.05	.41	50.00	13.50	0
5.00	7.78	.10	60.00	12.31	0
7.50	9.03	.02	70.00	10.32	0
10.00	10.00	0	80.00	7.71	0
15.00	11.50	0	90.00	4.39	0
20.00	12.71	0	95.00	2.41	0
25.00	13.51	0	100.00	.30	0

TABLE III.—ORDINATES, N. A. C. A. 86–M WING

Root section			Tip section		Root section			Tip section	
Station (% c from L. E.)	Upper (% c)	Lower (% c)	Upper (% c)	Lower (% c)	Station (% c from L. E.)	Upper (% c)	Lower (% c)	Upper (% c)	Lower (% c)
0	2.50	2.50	0	0	30.00	14.00	0	4.03	−4.03
1.25	4.85	.95	1.30	−1.30	40.00	14.11	0	4.00	−4.00
2.50	6.05	.41	1.74	−1.74	50.00	13.50	0	3.74	−3.74
5.00	7.78	.10	2.33	−2.33	60.00	12.31	0	3.30	−3.30
7.50	9.03	.02	2.74	−2.74	70.00	10.32	0	2.71	−2.71
10.00	10.00	0	3.05	−3.05	80.00	7.71	0	1.99	−1.99
15.00	11.50	0	3.49	−3.49	90.00	4.39	0	1.15	−1.15
20.00	12.71	0	3.78	−3.78	95.00	2.41	0	.69	−.69
25.00	13.51	0			100.00	.30	0	.20	−.20

TABLE IV.—STABLE-AUTOROTATION TESTS, BIPLANE WING, CLARK Y

Yaw=0°			Yaw=5°			Yaw=10°			Yaw=20°		
$\alpha°$	Positive rotation $\frac{pb}{2V}$	Negative rotation $\frac{pb}{2V}$	$\alpha°$	Positive rotation $\frac{pb}{2V}$	Negative rotation $\frac{pb}{2V}$	$\alpha°$	Positive rotation $\frac{pb}{2V}$	Negative rotation $\frac{pb}{2V}$	$\alpha°$	Positive rotation $\frac{pb}{2V}$	Negative rotation $\frac{pb}{2V}$
17	0.195	0.197	16	0.202	0	13	[1] 0.008	0	14	[1] 0.034	0
18	.233	.235	19	[1] .291	.261	18	[1] .271	0	16	[1] .154	0
20	[1] .291	[1] .278	20	[1] .310	.278	22	[1] .357	.280	18	[1] .250	0
24	[1] .371	[1] .360	21	[1] .336	[1] .306	26	[1] .448	.347	20	[1] .380	0
28	[1] .452	[1] .448	24	[1] .399	[1] .364	30	[1] .558	0	22	[1] .373	0
32	.483	.508	28	[1] .472	.452	34	[1] .724	0	24	[1] .416	0
36	.664	.718	32	[1] .584	.562	38	[1] .880	0	26	[1] .483	0
40	.842	.846	36	[1] .573	0	40	[1] .910	0	28	[1] .584	0
45	1.025	1.008	40	{[1] .222 / [1] 1.040}	.762	42	[1] .974	0	30	[1] .619	0
50	1.088	1.034				44	[1] 1.009	0	32	[1] .694	0
55	[1] 1.111	1.116	45	[1] 1.034	.955	46	[1] 1.060	0	34	[1] .754	0
60	[1] 1.192	1.254	50	[1] 1.117	1.055	48	[1] 1.105	0	36	[1] .830	0
65	[1] 1.296	1.283	55	[1] 1.198	1.131	50	[1] 1.168	0	38	[1] .890	0
70	[1] 1.272	1.292							40	[1] .929	0
75	{[1] 1.380 / [1] .027}	1.350							42	[1] .980	0
									44	[1] 1.043	0
									46	[1] 1.094	0
									48	[1] 1.163	0

[1] Self-starting.

TABLE V.—STABLE-AUTOROTATION TESTS, MONOPLANE WING, CLARK Y

Yaw=0°			Yaw=5°			Yaw=10°			Yaw=20°		
$\alpha°$	Positive rotation $\frac{pb}{2V}$	Negative rotation $\frac{pb}{2V}$	$\alpha°$	Positive rotation $\frac{pb}{2V}$	Negative rotation $\frac{pb}{2V}$	$\alpha°$	Positive rotation $\frac{pb}{2V}$	Negative rotation $\frac{pb}{2V}$	$\alpha°$	Positive rotation $\frac{pb}{2V}$	Negative rotation $\frac{pb}{2V}$
13.8	0	[1] 0.250	13	[1] 0.227	0	14	0.197	0	13	[1] 0.105	0
14.0	[1] .257	[1] .257	14	[1] .261	.244	15	[1] .278	0	20	[1] .362	0
18.0	[1] .306	[1] .306	20	[1] .332	.308	18	[1] .319	.255	28	[1] .500	0
24.0	[1] .323	[1] .341	24	[1] .360	.280	22	[1] .367	0	35	[1] .615	0
27.0	.291	.381	27	[1] .369	0	28	[1] .420	0	40	[1] .643	0
28.0	0	.236	30	[1] .315	0	35	[1] .215	0	50	[1] .323	0
28.6	0	.188	33	[1] .154	0	45	[1] .205	0	60	[1] .339	0
			35	[1] .138	0	55	[1] .218	0	70	[1] .369	0
			38	[1] .120	0	65	[1] .259	0	80	[1] .360	0
			42	[1] .110	0	75	[1] .293	0	85	[1] .321	0
			46	[1] .102	0	80	[1] .293	0	88	0	0
			50	[1] .102	0	85	[1] .188	0			
			55	[1] .198	0						

[1] Self-starting.

TABLE VI.—STABLE-AUTOROTATION TESTS, MONOPLANE WING, N. A. C. A. 84

Yaw=0°			Yaw=5°			Yaw=10°			Yaw=20°		
$\alpha°$	Positive rotation $\frac{pb}{2V}$	Negative rotation $\frac{pb}{2V}$	$\alpha°$	Positive rotation $\frac{pb}{2V}$	Negative rotation $\frac{pb}{2V}$	$\alpha°$	Positive rotation $\frac{pb}{2V}$	Negative rotation $\frac{pb}{2V}$	$\alpha°$	Positive rotation $\frac{pb}{2V}$	Negative rotation $\frac{pb}{2V}$
16	0.324	0.322	16	{[1] 0.060 / .335}	0.313	14	[1] 0.073	0	12	[1] 0.072	0
18	.360	.353	18	[1] .365	.342	16	[1] .165	0	14	[1] .118	0
20	.380	.365	20	[1] .387	.356	18	[1] .376	.311	16	[1] .313	0
22	[1] .394	[1] .387	22	[1] .414	.376	20	[1] .399	.335	18	[1] .376	0
24	[1] .417	[1] .405	24	[1] .437	.385	22	[1] .425	.347	20	[1] .414	0
28	[1] .419	[1] .419	26	[1] .452	.376	24	[1] .450	.351	22	[1] .450	0
30	[1] .405	[1] .405	28	[1] .470	.340	26	[1] .486	0	24	[1] .468	0
32	[1] .116	[1] .105	30	[1] .491	0	28	[1] .498	0	26	[1] .506	0
40	0	0	32	[1] .480	0	30	[1] .536	0	28	[1] .536	0
50	0	0	34	[1] .315	0	32	[1] .563	0	30	[1] .585	0
60	0	0	36	[1] .237	0	34	[1] .570	0	32	[1] .633	0
70	0	0	38	[1] .225	0	36	[1] .536	0	34	[1] .660	0
80	0	0	40	[1] .209	0	38	[1] .344	0	36	[1] .689	0
			50	[1] .124	0	40	[1] .301	0	38	[1] .718	0
									40	[1] .752	0
			60	[1] .132	0	45	[1] .263	0	42	[1] .779	0
									44	[1] .522	0
			70	[1] .165	0	50	[1] .254	0	46	[1] .486	0
									48	[1] .466	0
			80	0	0	60	[1] .265	0	50	[1] .450	0
									55	[1] .392	0
						70	[1] .306	0	60	[1] .392	0
									65	[1] .394	0
						75	[1] .315	0	70	[1] .409	0
									75	[1] .409	0
						80	[1] .313	0	80	[1] .432	0

[1] Self-starting.

TABLE VII.—STABLE-AUTOROTATION TESTS, MONOPLANE WING, N. A. C. A. 86–M

Yaw=0°			Yaw=5°			Yaw=10°			Yaw=20°		
$\alpha°$	Positive rotation $\frac{pb}{2v}$	Negative rotation $\frac{pb}{2v}$	$\alpha°$	Positive rotation $\frac{pb}{2v}$	Negative rotation $\frac{pb}{2v}$	$\alpha°$	Positive rotation $\frac{pb}{2v}$	Negative rotation $\frac{pb}{2v}$	$\alpha°$	Positive rotation $\frac{pb}{2v}$	Negative rotation $\frac{pb}{2v}$
12	0.118	0.121	13	[1] 0.192	0.145	13	[1] 0.171	0	12.5	0.094	0
13	[1] .190	[1] .193	14	[1] .234	.211	14	[1] .212	0	13	[1] .112	0
14	[1] .236	[1] .236	16	[1] .291	[1] .283	15	[1] .247	.207	14	[1] .147	0
16	[1] .294	[1] .289	18	[1] .325	[1] .319	16	[1] .272	.247	16	[1] .229	0
18	[1] .329	[1] .332	20	[1] .372	[1] .350	18	[1] .327	.296	18	[1] .292	0
20	[1] .365	[1] .359	22	[1] .405	[1] .381	20	[1] .372	[1] .334	20	[1] .338	0
22	[1] .399	[1] .387	24	[1] .437	.405	22	[1] .405	.370	22	[1] .394	0
22.5	[1] .405	[1] .401	26	[1] .479	0	24	[1] .432	.385	24	[1] .434	0
24	.434	.418	28	[1] .222	0	26	[1] .481	0	26	[1] .485	0
26	.465	0	30	[1] .168	0	28	[1] .445	0	28	[1] .535	0
30	0	0	35	[1] .144	0	30	[1] .465	0	30	[1] .557	0
			40	[1] .122	0	32	[1] .256	0	32	[1] .590	0
			45	[1] .113	0	34	[1] .234	0	35	[1] .628	0
			50	[1] .115	0	36	[1] .225	0	40	[1] .401	0
			55	[1] .131	0	38	[1] .225	0	45	[1] .367	0
			60	[1] .159	0	40	[1] .223	0	50	[1] .381	0
			65	[1] .185	0	45	[1] .231	0	55	[1] .394	0
			70	[1] .229	0	50	[1] .245	0	60	[1] .399	0
			75	[1] .254	0	55	[1] .256	0	65	[1] .403	0
			80	[1] .272	0	60	[1] .265	0	70	[1] .403	0
						65	[1] .276	0	75	[1] .407	0
						70	[1] .296	0	80	[1] .392	0
						75	[1] .307	0			
						80	[1] .318	0			

[1] Self-starting.

TABLE VIII.—ROLLING-MOMENT TESTS, BIPLANE WING, CLARK Y

[Yaw=0°]

$\alpha=0°$				$\alpha=40°$			
Positive rotation		Negative rotation		Positive rotation		Negative rotation	
$\frac{pb}{2V}$	C_λ	$\frac{pb}{2V}$	C_λ	$\frac{pb}{2V}$	C_λ	$\frac{pb}{2V}$	C_λ
0.046	−0.0136	0.044	0.0187	0.100	−0.0039	0.153	0.0069
.076	−.0247	.058	.0237	.207	−.0077	.248	+.0096
.113	−.0376	.094	.0358	.738	+.0072	.705	−.0050
				.820	+.0037	.815	−.0021
				1.015	−.0185	1.015	+.0217
$\alpha=18°$				$\alpha=45°$			
0.175	+0.0080	0.183	−0.0082	0.116	−0.0029	0.103	0.0043
.293	−.0091	.295	+.0107	.216	−.0054	.195	.0071
.371	−.0238	.375	.0286	.945	+.0083	.285	+.0077
.436	−.0392	.408	.0348	1.017	+.0007	.885	−.0065
				1.074	−.0131	.990	−.0004
				1.140	−.0263	1.079	+.0154
$\alpha=30°$				$\alpha=55°$			
0.347	+0.0078	0.432	−0.0086	1.027	0.0090	1.025	−0.0084
.530	−.0050	.533	+.0037	1.094	.0058	1.148	+.0032
.626	−.0163	.647	.0208	1.204	.0000		
.710	−.0284	.718	.0315				
$\alpha=35°$				$\alpha=70°$			
0.170	−0.0049	0.140	+0.0054	1.198	0.0091	1.144	−0.0075
.587	+.0013	.673	−.0015	1.255	.0041	1.228	−.0036
.682	−.0024	.770	+.0087	1.327	.0006	1.310	+.0004
.750	−.0084	.845	.0202				
.817	−.0154						

TABLE IX.—ROLLING-MOMENT TESTS, BIPLANE WING, CLARK Y

[Yaw=5°]

$\alpha=0°$			
Positive rotation		Negative rotation	
$\frac{pb}{2V}$	C_λ	$\frac{pb}{2V}$	C_λ
0.063	−0.0215	0.032	0.0130
.085	−.0298	.058	.0221
.108	−.0367	.100	.0371
$\alpha=19°$			
0.126	0.0269	0.218	−0.0056
.168	.0224	.280	+.0030
.261	+.0072	.371	.0187
.323	−.0059	.433	.0313
.388	−.0194		
.431	−.0300		
$\alpha=25°$			
0.169	0.0288	0.216	−0.0199
.246	.0236	.336	−.0078
.371	+.0085	.436	+.0078
.479	−.0099	.522	.0235
.541	−.0215		
$\alpha=30°$			
0.433	0.0086	0.403	−0.0077
.518	+.0015	.531	+.0032
.632	−.0095	.649	.0168
.720	−.0249	.746	.0316
$\alpha=35°$			
0.072	0.0065	0.178	0.0166
.224	.0072	.332	.0107
.507	.0142	.527	.0055
.653	+.0052	.643	.0053
.750	−.0029	.885	.0229
.828	−.0124		
.905	−.0256		

$\alpha=40°$			
Positive rotation		Negative rotation	
$\frac{pb}{2V}$	C_λ	$\frac{pb}{2V}$	C_λ
0.057	0.0056	0.192	0.0164
.145	+.0021	.274	+.0181
.233	−.0003	.600	−.0001
.697	+.0187	.716	−.0010
.828	+.0097	.945	−.0073
.934	−.0033		
1.068	−.0341		
$\alpha=45°$			
0.100	0.0038	0.196	0.0125
.156	.0023	.287	+.0141
.224	.0005	.870	−.0081
.787	.0227	.970	+.0014
.992	.0102	1.088	.0103
1.048	+.0007		
1.090	−.0120		
$\alpha=50°$			
0.593	0.0212	0.159	+0.0073
1.035	+.0109	.755	−.0174
1.153	−.0030	.920	−.0108
1.208	−.0099	1.084	−.0046
		1.190	−.0156
$\alpha=55°$			
0.828	0.0212	1.026	−0.0107
.935	.0172	1.143	+.0010
1.040	.0119		
1.100	.0082		
1.209	.0002		

TABLE X.—ROLLING-MOMENT TESTS, BIPLANE WING, CLARK Y

[Yaw=10°]

$\alpha=0°$			
Positive rotation		Negative rotation	
$\frac{pb}{2V}$	C_λ	$\frac{pb}{2V}$	C_λ
0.037	−0.0133	0.031	0.0110
.060	−.0212	.068	.0241
.097	−.0337	.094	.0329
$\alpha=19°$			
0.160	0.0249	0.227	0.0029
.261	+.0064	.315	.0132
.364	−.0166	.438	.0330
.410	−.0265		
$\alpha=25°$			
0.233	0.0296	0.211	−0.0082
.375	+.0101	.360	+.0011
.485	−.0104	.472	.0146
.531	−.0191	.548	.0262
.571	−.0270		
$\alpha=30°$			
0.285	0.0267	0.072	0.0257
.380	.0165	.094	.0262
.494	+.0086	.453	.0024
.647	−.0099	.533	.0071
.755	−.0296	.643	.0173
		.735	.0274

$\alpha=35°$			
Positive rotation		Negative rotation	
$\frac{pb}{2V}$	C_λ	$\frac{pb}{2V}$	C_λ
0.511	0.0217	0.138	0.0256
.688	.0095	.224	.0274
.742	+.0044	.532	.0136
.838	−.0092	.744	.0037
.896	−.0214	.850	.0131
		.899	.0212
$\alpha=40°$			
0.695	0.0266	0.085	0.0200
.886	+.0111	.215	.0247
.962	−.0039	.300	.0260
1.057	−.0295	.761	.0035
		.869	.0044
		.923	.0038
		1.046	.0168
		1.110	.0351
$\alpha=45°$			
0.726	0.0318	0.151	0.0172
.817	.0269	.246	+.0199
.990	+.0103	.895	−.0027
1.083	−.0080	.970	+.0035
1.186	−.0313	1.078	.0097
		1.142	.0192
$\alpha=50°$			
0.696	0.0265	0.201	+0.0121
.824	.0252	.892	−.0094
1.065	.0104	1.012	−.0011
1.110	+.0063	1.149	+.0117
1.197	−.0028		

TABLE XI.—ROLLING-MOMENT TESTS, BIPLANE WING, CLARK Y

[Yaw=20°]

$\alpha=0°$			
Positive rotation		Negative rotation	
$\frac{pb}{2V}$	C_λ	$\frac{pb}{2V}$	C_λ
0.047	−0.0149	0.050	0.0146
.079	−.0239	.090	.0267
.110	−.0335	.119	.0355
$\alpha=15°$			
0.072	−0.0034	0.043	0.0235
.140	−.0128	.075	.0314
.252	−.0226	.098	.0377
.317	−.0335		
$\alpha=20°$			
0.135	0.0335		
.166	.0278		
.203	.0207		
.280	+.0054		
.310	−.0016		
.362	−.0105		
.436	−.0246		
$\alpha=25°$			
0.246	0.0357		
.285	.0287		
.418	+.0087		
.520	−.0114		
.561	−.0209		
.638	−.0360		
$\alpha=30°$			
0.287	0.0376		
.330	.0340		
.462	.0227		
.573	+.0083		
.638	−.0009		
.703	−.0127		

$\alpha=35°$			
Positive rotation		Negative rotation	
$\frac{pb}{2V}$	C_λ	$\frac{pb}{2V}$	C_λ
0.485	0.0326		
.563	.0287		
.730	+.0120		
.858	−.0117		
.945	−.0342		
$\alpha=40°$			
0.297	0.0272	0.267	0.0372
.703	.0327	1.073	.0122
.800	.0263		
.889	+.0108		
.991	−.0080		
1.080	−.0322		
$\alpha=45°$			
0.595	0.0370	0.179	0.0267
.824	.0351	.313	.0290
1.030	+.0116	.905	.0029
1.115	−.0105	1.010	.0096
		1.078	.0154
$\alpha=50°$			
0.714	0.0347	0.210	0.0207
.946	.0260	.950	.0010
1.170	+.0115	1.089	.0093
1.280	−.0101		

TABLE XII.—ROLLING-MOMENT TESTS, MONOPLANE WING, CLARK Y

[Yaw=0°]

$\alpha=0°$			
Positive rotation		Negative rotation	
$\frac{pb}{2V}$	C_λ	$\frac{pb}{2V}$	C_λ
0.078	−0.0351	0.082	0.0316
.147	−.0623	.142	.0567
.213	−.0927	.196	.0795
$\alpha=14°$			
0.080	−0.0096	0.063	0.0107
.085	−.0087	.101	+.0134
.208	+.0117	.231	−.0059
.239	−.0054	.306	+.0117
.250	+.0011	.401	.0365
.255	−.0011	.477	.0633
.306	−.0040		
.309	−.0152		
.477	−.0641		
$\alpha=20°$			
0.129	0.0308	0.136	−0.0316
.170	.0279	.244	−.0180
.246	+.0163	.291	−.0075
.339	−.0031	.380	+.0124
.494	−.0423	.560	.0578
.632	−.0791		
$\alpha=25°$			
0.048	−0.0010	0.044	−0.0011
.265	+.0065	.278	−.0085
.393	−.0096	.371	+.0037
.582	−.0457	.665	.0648

$\alpha=28°$			
Positive rotation		Negative rotation	
$\frac{pb}{2V}$	C_λ	$\frac{pb}{2V}$	C_λ
0.074	−0.0041	0.066	0.0023
.237	−.0031	.227	+.0018
.338	−.0050	.306	−.0002
.412	−.0117	.412	+.0079
.552	−.0313	.570	.0315
.790	−.0934	.703	.0617
$\alpha=30°$			
0.104	−0.0059	0.105	0.0050
.263	−.0062	.227	.0047
.302	−.0079	.315	.0060
.362	−.0096	.362	.0090
.411	−.0127	.399	.0085
.451	−.0156	.555	.0242
.574	−.0294	.688	.0503
.651	−.0468		
$\alpha=40°$			
0.095	−0.0074	0.073	0.0043
.239	−.0149	.170	.0089
.433	−.0268	.285	.0165
.680	−.0402	.449	.0265
		.729	.0415

TABLE XIII.—ROLLING-MOMENT TESTS, MONOPLANE WING, CLARK Y

[Yaw=5°]

$\alpha=0°$			
Positive rotation		Negative rotation	
$\frac{pb}{2V}$	C_λ	$\frac{pb}{2V}$	C_λ
0.082	−0.0371	0.078	0.0302
.153	−.0665	.138	.0533
.203	−.0875	.185	.0735
$\alpha=13°$			
0.073	−0.0099	0.055	0.0146
.137	−.0143	.120	.0348
.220	−.0008	.246	.0080
.269	−.0099	.257	.0085
.276	−.0122	.278	.0124
.379	−.0410	.280	.0180
.498	−.0796	.310	.0192
.591	−.1137	.332	.0235
		.379	.0370
		.392	.0405
		.466	.0628
$\alpha=20°$			
0.128	0.0418	0.178	−0.0194
.218	.0279	.255	−.0103
.284	.0128	.349	+.0086
.332	+.0025	.610	.0717
.444	−.0274		
.617	−.0780		
$\alpha=27°$			
0.067	0.0086	0.097	0.0135
.246	.0104	.317	.0061
.371	+.0006	.432	.0192
.513	−.0229	.660	.0564
.665	−.0561		

$\alpha=33°$			
Positive rotation		Negative rotation	
$\frac{pb}{2V}$	C_λ	$\frac{pb}{2V}$	C_λ
0.075	0.0050	0.089	0.0150
.110	+.0031	.222	.0208
.190	−.0026	.360	.0228
.345	−.0056	.496	.0265
.473	−.0109	.625	.0375
.725	−.0418	.749	.0542
$\alpha=50°$			
0.095	+0.0004	0.132	0.0127
.208	−.0048	.224	.0172
.315	−.0117	.328	.0201
.436	−.0203	.468	.0323
.550	−.0286	.676	.0440
.638	−.0349	.835	.0540
$\alpha=65°$			
0.125	+0.0002	0.138	0.0073
.231	−.0017	.274	.0086
.319	−.0054	.408	.0123
.453	−.0118	.500	.0147
.585	−.0179	.692	.0237
.695	−.0232		
$\alpha=80°$			
0.139	+0.0002	0.166	0.0012
.261	−.0002	.291	.0013
.407	−.0021	.485	.0016
.550	−.0035	.623	.0021
.722	−.0039	.865	.0016
$\alpha=85°$			
0.132	−0.0003	0.159	−0.0002
.280	−.0006	.328	−.0002
.447	−.0011	.589	−.0005
.583	−.0015	.780	−.0007
.790	−.0017	.955	−.0014

TABLE XIV.—ROLLING-MOMENT TESTS, MONOPLANE WING, CLARK Y

[Yaw=10°]

$\alpha=0°$			
Positive rotation		Negative rotation	
$\frac{pb}{2V}$	C_λ	$\frac{pb}{2V}$	C_λ
0.060	−0.0279	0.103	0.0405
.110	−.0470	.113	.0430
.147	−.0625	.176	.0682
$\alpha=15°$			
0.163	0.0271	0.047	0.0321
.235	+.0117	.298	.0114
.285	−.0010	.382	.0283
.460	−.0521	.480	.0556
.528	−.0780		
$\alpha=22°$			
0.201	0.0324	0.220	0.0005
.311	+.0137	.332	.0063
.455	−.0204	.436	.0260
.580	−.0529	.563	.0545
$\alpha=28°$			
0.176	0.0176	0.108	0.0232
.222	.0159	.210	.0210
.281	.0131	.373	.0191
.410	+.0023	.520	.0350
.628	−.0393	.690	.0607
.733	−.0692		
$\alpha=35°$			
0.052	0.0121	0.108	0.0220
.084	.0097	.214	.0281
.160	+.0032	.434	.0346
.257	−.0034	.710	.0482
.490	−.0055		
.645	−.0135		
.835	−.0544		

$\alpha=50°$			
Positive rotation		Negative rotation	
$\frac{pb}{2V}$	C_λ	$\frac{pb}{2V}$	C_λ
0.062	0.0062	0.140	0.0179
.134	+.0027	.272	.0237
.237	−.0021	.574	.0415
.393	−.0130	.662	.0465
.516	−.0214		
.750	−.0322		
$\alpha=65°$			
0.093	0.0042	0.147	0.0098
.222	+.0011	.371	.0119
.410	−.0076	.621	.0202
.595	−.0173	.811	.0272
.761	−.0230		
1.000	−.0277		
$\alpha=80°$			
0.146	+0.0010	0.148	0.0017
.302	−.0002	.272	.0014
.483	−.0021	.466	.0012
.677	−.0035	.630	.0013
.855	−.0036	.863	.0021
.992	−.0035		
$\alpha=85°$			
0.172	−0.0004	0.233	+0.0002
.319	−.0005	.453	−.0002
.555	−.0004	.680	+.0003
.696	−.0013	.879	−.0008
.830	−.0011		

TABLE XV.—ROLLING-MOMENT TESTS, MONOPLANE WING, CLARK Y

[Yaw=20°]

$\alpha=0°$			
Positive rotation		Negative rotation	
$\frac{pb}{2V}$	C_λ	$\frac{pb}{2V}$	C_λ
0.111	−0.0447	0.101	0.0302
.169	−.0650	.166	.0525
.255	−.0966	.210	.0701
$\alpha=15°$			
0.108	0.0420	0.055	0.0514
.224	+.0133	.147	.0575
.287	−.0031	.358	.0372
.401	−.0363	.467	.0493
.516	−.0709	.540	.0634
$\alpha=20°$			
0.108	0.0615	0.240	0.0254
.233	.0332	.341	.0264
.317	+.0125	.546	.0510
.432	−.0174	.676	.0827
.607	−.0684	.751	.1040
$\alpha=28°$			
0.167	0.0487	0.135	0.0443
.279	.0367	.452	.0355
.434	+.0173	.617	.0541
.609	−.0294		
.747	−.0681		
$\alpha=35°$			
0.087	0.0223	0.133	0.0382
.215	.0132	.264	.0440
.465	.0168	.534	.0514
.596	+.0030	.700	.0600
.715	−.0179		

$\alpha=45°$			
Positive rotation		Negative rotation	
$\frac{pb}{2V}$	C_λ	$\frac{pb}{2V}$	C_λ
0.107	0.0149	0.158	0.0318
.235	+.0062	.354	.0392
.399	−.0028	.499	.0430
.525	−.0106	.660	.0551
.805	−.0089		
$\alpha=60°$			
0.122	0.0098	0.128	0.0185
.212	.0060	.246	.0218
.315	+.0018	.505	.0205
.405	−.0034	.718	.0321
.655	−.0174		
.896	−.0318		
$\alpha=75°$			
0.145	0.0049	0.135	0.0077
.278	+.0032	.274	.0078
.418	−.0013	.612	.0065
.522	−.0029	.743	.0086
.808	−.0058		
$\alpha=85°$			
0.187	0.0013	0.183	0.0015
.317	.0009	.444	.0011
.585	.0004	.600	.0009
.651	.0000	.740	+.0005
1.010	.0022	.905	−.0008

TABLE XVI.—ROLLING-MOMENT TESTS, MONOPLANE WING, N. A. C. A. 84

[Yaw=0°]

$\alpha=-6°$			
Positive rotation		Negative rotation	
$\frac{pb}{2V}$	C_λ	$\frac{pb}{2V}$	C_λ
0.063	−0.0225	0.056	0.0233
.109	−.0411	.091	.0385
.153	−.0590	.120	.0498
$\alpha=0°$			
0.037	−0.0016	0.039	0.0206
.073	−.0312	.067	.0324
.143	−.0596	.088	.0407
$\alpha=6°$			
0.070	−0.0277	0.071	0.0330
.104	−.0404	.111	.0493
.128	−.0515		
$\alpha=12°$			
0.067	−0.0204	0.071	0.0259
.127	−.0417	.119	.0392
.190	−.0545	.149	.0471
$\alpha=16°$			
0.061	−0.0113	0.086	0.0155
.114	−.0180	.194	+.0120
.269	+.0139	.261	−.0134
.378	−.0098	.351	+.0080
.392	−.0146	.359	+.0108
$\alpha=18°$			
0.204	0.0391	0.213	−0.0351
.233	.0327	.233	−.0312
.319	+.0124	.319	−.0113
.392	−.0067	.407	+.0145
$\alpha=20°$			
0.172	0.0417	0.177	−0.0425
.223	.0366	.227	−.0354
.247	.0325	.263	−.0296
.341	+.0120	.335	−.0117
.423	−.0093	.407	+.0073

$\alpha=22°$			
Positive rotation		Negative rotation	
$\frac{pb}{2V}$	C_λ	$\frac{pb}{2V}$	C_λ
0.157	0.0493	0.112	−0.0460
.215	.0426	.182	−.0437
.245	.0371	.219	−.0382
.263	.0326	.253	−.0333
.341	+.0142	.329	−.0149
.417	−.0014	.408	+.0041
.453	−.0117	.478	.0213
$\alpha=24°$			
0.184	0.0364	0.210	−0.0360
.255	.0321	.245	−.0318
.366	.0143	.341	−.0138
.423	+.0020	.423	+.0029
.505	−.0160	.507	.0208
$\alpha=26°$			
0.351	0.0134	0.351	−0.0123
.423	+.0009	.423	−.0008
.470	−.0073	.478	+.0107
.555	−.0260	.568	+.0304
$\alpha=30°$			
0.404	+0.0017	0.404	−0.0010
.462	−.0032	.449	+.0049
.554	−.0161	.547	.0180
$\alpha=35°$			
0.164	−0.0037	0.164	0.0042
.269	−.0093	.255	.0095
.407	−.0122	.394	.0118
.519	−.0146	.513	.0146

TABLE XVII.—ROLLING-MOMENT TESTS, MONOPLANE WING, N. A. C. A. 84

[Yaw=10°]

$\alpha=-6°$			
Positive rotation		Negative rotation	
$\frac{pb}{2V}$	C_λ	$\frac{pb}{2V}$	C_λ
0.046	−0.0164	0.057	0.0248
.061	−.0222	.085	.0357
.085	−.0259	.118	.0498
.112	−.0435		

$\alpha=0°$			
0.054	−0.0203	0.051	0.0273
.080	−.0308	.085	.0415
.138	−.0538	.120	.0545

$\alpha=6°$			
0.064	−0.0202	0.060	0.0322
.093	−.0316	.099	.0468
.138	−.0492	.128	.0587

$\alpha=12°$			
0.069	−0.0088	0.071	0.0368
.095	−.0161	.115	.0495
.142	−.0293	.144	.0585
.190	−.0441		

$\alpha=16°$			
0.088	+0.0074	0.117	0.0443
.189	−.0043	.343	.0111
.270	+.0142	.421	.0279
.333	−.0028	.503	.0533
.366	−.0121		
.405	−.0225		

$\alpha=18°$			
0.170	0.0505	0.335	0.0036
.247	.0345	.462	.0325
.329	.0125	.527	.0527
.378	−.0015		
.400	−.0100		
.492	−.0319		

$\alpha=20°$			
0.136	0.0625	0.349	0.0023
.186	.0527	.468	.0281
.235	.0432	.540	.0472
.278	.0327		
.353	+.0124		
.447	−.0124		
.490	−.0237		

$\alpha=22°$			
Positive rotation		Negative rotation	
$\frac{pb}{2V}$	C_λ	$\frac{pb}{2V}$	C_λ
0.099	0.0676	0.272	−0.0109
.239	.0448	.351	+.0002
.290	.0351	.419	.0136
.378	.0129	.468	.0249
.425	+.0019	.527	.0382
.507	−.0222		

$\alpha=24°$			
0.132	0.0567	0.353	0.0005
.253	.0423	.502	.0262
.316	.0310	.560	.0411
.400	+.0129		
.505	−.0127		
.550	−.0243		

$\alpha=26°$			
0.168	0.0438	0.327	0.0003
.243	.0404	.429	.0120
.300	.0327	.502	.0244
.417	+.0139	.590	.0408
.576	−.0233		

$\alpha=30°$			
0.046	0.0304	0.115	0.0284
.116	.0268	.337	.0126
.447	+.0143	.425	.0179
.562	−.0050	.543	.0294
.615	−.0149	.630	.0413

$\alpha=35°$			
0.219	0.0108	0.084	0.0269
.535	+.0027	.147	.0277
.641	−.0044	.221	.0297
.690	−.0116	.298	.0303
		.421	.0301
		.540	.0337
		.654	.0411

TABLE XVIII.—ROLLING-MOMENT TESTS, MONOPLANE WING, N. A. C. A. 86–M

[Yaw=0°]

$\alpha=0°$			
Positive rotation		Negative rotation	
$\frac{pb}{2V}$	C_λ	$\frac{pb}{2V}$	C_λ
0.069	−0.0319	0.069	0.0343
.103	−.0465	.109	.0498
.129	−.0570	.160	.0708
.165	−.0732		

$\alpha=10°$			
0.084	−0.0214	0.069	0.0208
.209	−.0282	.077	.0212
.272	−.0401	.156	.0221
.327	−.0546	.240	.0330
.378	−.0660	.321	.0506
		.361	.0589

$\alpha=15°$			
0.201	+0.0131	0.200	−0.0133
.287	−.0044	.287	+.0055
.329	−.0147	.358	.0255
.389	−.0303	.438	.0492
.530	−.0746	.487	.0655

$\alpha=20°$			
0.307	+0.0152	0.301	−0.0141
.376	−.0031	.376	+.0036
.418	−.0113	.445	.0219
.487	−.0313	.505	.0398
.579	−.0601	.583	.0628
.601	−.0685		

$\alpha=25°$			
0.053	−0.0025	0.115	+0.0046
.374	+.0158	.323	−.0078
.445	+.0013	.405	+.0002
.516	−.0158	.478	.0132
.581	−.0315	.554	.0287
.625	−.0467	.623	.0464
.677	−.0620		

$\alpha=30°$			
0.097	−0.0041	0.132	0.0080
.221	−.0105	.233	.0128
.369	−.0146	.521	.0205
.525	−.0213	.625	.0349
.637	−.0415	.699	.0504
.695	−.0512		
.752	−.0617		

$\alpha=35°$			
Positive rotation		Negative rotation	
$\frac{pb}{2V}$	C_λ	$\frac{pb}{2V}$	C_λ
0.102	−0.0052	0.139	0.0105
.236	−.0127	.247	.0154
.383	−.0242	.338	.0225
.547	−.0274	.541	.0299
.679	−.0299	.730	.0413
.739	−.0379	.788	.0518
.812	−.0531		

$\alpha=40°$			
0.158	−0.0094	0.139	0.0103
.278	−.0151	.280	.0166
.367	−.0222	.340	.0220
.577	−.0376	.429	.0284
.610	−.0390	.498	.0334
.748	−.0435	.552	.0370
.832	−.0497	.719	.0426
		.792	.0475

$\alpha=50°$			
0.096	−0.0044	0.138	0.0080
.222	−.0103	.236	.0122
.311	−.0127	.331	.0151
.472	−.0246	.448	.0242
.677	−.0385	.532	.0303
.757	−.0453	.695	.0409
		.795	.0458

$\alpha=65°$			
0.196	−0.0031	0.181	0.0047
.314	−.0057	.301	.0065
.443	−.0123	.450	.0141
.541	−.0168	.570	.0189
.661	−.0217	.704	.0241
.760	−.0256		

$\alpha=80°$			
0.294	−0.0001	0.311	0.0014
.432	−.0016	.416	.0023
.543	−.0027	.515	.0033
.605	−.0032	.672	.0046
.695	−.0038		

TABLE XIX.—ROLLING-MOMENT TESTS, MONOPLANE WING, N. A. C. A. 86-M

[Yaw=5°]

$\alpha=0°$			
Positive rotation		Negative rotation	
$\frac{pb}{2V}$	C_λ	$\frac{pb}{2V}$	C_λ
0.049	−0.0233	0.048	0.0249
.099	−.0442	.074	.0358
.128	−.0561	.110	.0506
.163	−.0706	.159	.0690
$\alpha=10°$			
0.152	−0.0196	0.124	0.0299
.256	−.0351	.258	.0390
.332	−.0548	.278	.0427
.401	−.0751	.347	.0580
		.394	.0708
$\alpha=15°$			
0.192	+0.0143	0.167	−0.0135
.267	−.0009	.272	+.0045
.327	−.0167	.347	.0215
.372	−.0306	.385	.0341
.430	−.0464	.432	.0481
.463	−.0586	.494	.0663
$\alpha=20°$			
0.197	0.0401	0.208	−0.0251
.312	+.0153	.285	−.0148
.392	−.0060	.372	+.0040
.432	−.0168	.418	.0168
.568	−.0597	.539	.0500
		.597	.0687
$\alpha=25°$			
0.325	0.0283	0.316	−0.0049
.403	+.0131	.396	+.0019
.560	−.0258	.521	.0249
.632	−.0498	.636	.0531
$\alpha=30°$			
0.042	+0.0084	0.083	0.0158
.225	−.0034	.186	.0207
.412	−.0060	.307	.0231
.483	−.0096	.450	.0241
.574	−.0233	.561	.0315
.659	−.0391	.670	.0491
.715	−.0507		

$\alpha=35°$			
Positive rotation		Negative rotation	
$\frac{pb}{2V}$	C_λ	$\frac{pb}{2V}$	C_λ
0.225	−0.0055	0.121	0.0176
.367	−.0170	.263	.0247
.521	−.0196	.381	.0308
.648	−.0274	.552	.0377
.750	−.0421	.699	.0466
$\alpha=40°$			
0.225	−0.0056	0.135	0.0175
.329	−.0141	.240	.0232
.465	−.0237	.354	.0281
.568	−.0301	.454	.0366
.736	−.0357	.570	.0445
		.681	.0482
$\alpha=50°$			
0.296	−0.0047	0.167	0.0150
.352	−.0111	.247	.0189
.463	−.0193	.363	.0227
.543	−.0247	.501	.0335
.670	−.0326	.681	.0452
.768	−.0408	.793	.0513
$\alpha=65°$			
0.314	−0.0029	0.243	0.0091
.443	−.0089	.374	.0118
.548	−.0146	.459	.0153
.668	−.0196	.597	.0220
.760	−.0235	.697	.0255
		.797	.0292
$\alpha=80°$			
0.418	−0.0014	0.412	0.0040
.650	−.0029	.547	.0053
.804	−.0027	.708	.0073
		.795	.0075

TABLE XX.—ROLLING-MOMENT TESTS, MONOPLANE WING, N. A. C. A. 86-M

[Yaw=10°]

$\alpha=0°$			
Positive rotation		Negative rotation	
$\frac{pb}{2V}$	C_λ	$\frac{pb}{2V}$	C_λ
0.049	−0.0211	0.046	0.0240
.093	−.0391	.067	.0326
.139	−.0584	.102	.0450
.173	−.0711	.155	.0659
$\alpha=10°$			
0.056	−0.0158	0.065	−0.0166
.146	−.0201	.073	+.0244
.201	−.0273	.113	.0340
.261	−.0392	.265	.0485
.307	−.0508	.354	.0647
.354	−.0645		
$\alpha=15°$			
0.077	0.0252	0.115	−0.0087
.175	+.0149	.225	+.0028
.278	−.0084	.287	.0128
.327	−.0208	.361	.0283
.385	−.0371	.416	.0420
.425	−.0516	.463	.0569
.461	−.0654		
$\alpha=20°$			
0.197	0.0401	0.202	−0.0230
.312	+.0129	.258	−.0144
.452	−.0239	.334	+.0005
.501	−.0369	.458	.0293
.552	−.0575	.518	.0445
		.565	.0605
$\alpha=25°$			
0.153	0.0131	0.369	0.0044
.392	.0153	.465	.0170
.458	.0005	.577	.0401
.577	.0338	.652	.0615
.625	.0520		
$\alpha=30°$			
0.122	0.0115	0.108	0.0269
.443	+.0017	.243	.0325
.512	−.0071	.327	.0330
.612	−.0270	.470	.0318
.712	−.0498	.599	.0422
		.688	.0565

$\alpha=35°$			
Positive rotation		Negative rotation	
$\frac{pb}{2V}$	C_λ	$\frac{pb}{2V}$	C_λ
0.098	−0.0110	0.104	0.0254
.260	−.0024	.222	.0325
.347	−.0086	.314	.0354
.463	−.0086	.443	.0417
.561	−.0125	.565	.0455
.672	−.0233	.683	.0521
$\alpha=40°$			
0.083	+0.0105	0.091	0.0221
.234	−.0007	.227	.0304
.331	−.0081	.361	.0341
.436	−.0156	.458	.0432
.583	−.0219	.581	.0508
.688	−.0261	.668	.0537
.760	−.0315		
$\alpha=50°$			
0.062	+0.0088	0.134	0.0198
.265	−.0015	.240	.0240
.430	−.0132	.325	.0268
.574	−.0219	.441	.0317
.683	−.0295	.588	.0438
.779	−.0375	.692	.0502
		.788	.0559
$\alpha=65°$			
0.329	−0.0017	0.179	0.0120
.452	−.0075	.296	.0124
.583	−.0131	.458	.0165
.690	−.0171	.597	.0219
.799	−.0200	.721	.0275
$\alpha=80°$			
0.316	+0.0004	0.234	0.0030
.458	−.0017	.365	.0030
.574	−.0027	.450	.0037
.672	−.0036	.583	.0044
.805	−.0029	.699	.0054
		.852	.0054

TABLE XXI.—ROLLING-MOMENT TESTS, MONOPLANE WING, N. A. C. A. 86–M

[Yaw=20°]

α=0°				α=35°			
Positive rotation		Negative rotation		Positive rotation		Negative rotation	
$\frac{pb}{2V}$	C_λ	$\frac{pb}{2V}$	C_λ	$\frac{pb}{2V}$	C_λ	$\frac{pb}{2V}$	C_λ
0.054	−0.0181	0.061	0.0278	0.225	0.0155	0.137	0.0430
.089	−.0297	.104	.0426	.532	+.0057	.316	.0507
.131	−.0452	.145	.0553	.681	−.0105	.515	.0541
.174	−.0596	.199	.0737	.748	−.0242	.712	.0627
.205	−.0715			.804	−.0373		
α=10°				α=40°			
0.071	−0.0150	0.065	0.0240	0.195	0.0130	0.133	0.0383
.159	−.0251	.101	.0341	.396	+.0007	.238	.0433
.225	−.0380	.151	.0485	.461	−.0020	.378	.0488
.274	−.0480	.274	.0680	.581	−.0064	.556	.0550
.343	−.0655			.688	−.0088	.688	.0633
				.799	−.0195		
				.855	−.0329		
α=15°				α=50°			
0.104	+0.0118	0.142	0.0238	0.168	0.0123	0.186	0.0322
.214	−.0025	.238	.0285	.398	.0000	.303	.0358
.307	−.0217	.303	.0349	.465	−.0043	.476	.0372
.365	−.0368	.381	.0449	.595	−.0136	.614	.0491
.410	−.0491	.461	.0550	.699	−.0203	.708	.0540
.445	−.0618			.821	−.0264		
α=20°				α=65°			
0.197	0.0287	0.222	0.0035	0.095	0.0117	0.178	0.0186
.287	.0122	.314	.0139	.414	+.0012	.305	.0192
.327	+.0031	.372	.0207	.574	−.0058	.472	.0192
.458	−.0329	.447	.0290	.670	−.0096	.596	.0238
.528	−.0572	.568	.0568	.792	−.0136	.681	.0277
						.776	.0318
α=25°				α=80°			
0.146	0.0449	0.127	0.0442	0.410	+0.0009	0.182	0.0055
.285	.0367	.214	.0455	.534	−.0001	.327	.0050
.403	+.0173	.372	.0264	.699	−.0006	.461	.0054
.477	−.0044	.503	0.0328	.790	−.0009	.587	.0057
.521	−.0217	.619	.0521			.705	.0070
.601	−.0518	.688	.0680			.830	.0071
α=30°							
0.085	0.0308	0.094	0.0435				
.481	.0160	.222	.0507				
.550	+.0027	.338	.0516				
.699	−.0330	.572	.0473				
.767	−.0522	.681	.0583				

TABLE XXII.—TEST ANGLES OF ATTACK AND YAW IN N. A. C. A. STANDARD EQUIVALENTS

Angle of attack (test)	Angle of attack (std.)	Angle of yaw (test)	Angle of yaw (std.)	Angle of attack (test)	Angle of attack (std.)	Angle of yaw (test)	Angle of yaw (std.)
°	° ′	°	° ′	°	° ′	°	° ′
0	0 0	10	10 0	0	0 0	20	20 0
15	14 55	10	9 40	15	14 25	20	19 15
30	29 45	10	8 40	30	29 10	20	17 20
45	44 38	10	7 0	45	43 45	20	14 5
60	59 40	10	4 50	60	59 5	20	10 10
75	74 50	10	2 24	75	74 45	20	5 35
90	90 0	10	0 0	90	90 0	20	0 0

U. S. GOVERNMENT PRINTING OFFICE: 1931

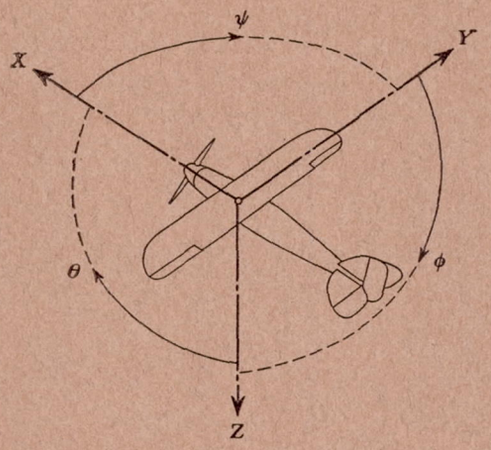

Positive directions of axes and angles (forces and moments) are shown by arrows

Axis		Force (parallel to axis) symbol	Moment about axis			Angle		Velocities	
Designation	Symbol		Designation	Symbol	Positive direction	Designation	Symbol	Linear (component along axis)	Angular
Longitudinal	X	X	rolling	L	$Y \longrightarrow Z$	roll	ϕ	u	p
Lateral	Y	Y	pitching	M	$Z \longrightarrow X$	pitch	θ	v	q
Normal	Z	Z	yawing	N	$X \longrightarrow Y$	yaw	ψ	w	r

Absolute coefficients of moment

$$C_l = \frac{L}{qbS} \qquad C_m = \frac{M}{qcS} \qquad C_n = \frac{N}{qbS}$$

Angle of set of control surface (relative to neutral position), δ. (Indicate surface by proper subscript.)

4. PROPELLER SYMBOLS

D, Diameter.

p, Geometric pitch.

p/D, Pitch ratio.

V', Inflow velocity.

V_s, Slipstream velocity.

T, Thrust, absolute coefficient $C_T = \frac{T}{\rho n^2 D^4}$

Q, Torque, absolute coefficient $C_Q = \frac{Q}{\rho n^2 D^5}$

P, Power, absolute coefficient $C_P = \frac{P}{\rho n^3 D^5}$.

C_S, Speed power coefficient $= \sqrt[5]{\frac{\rho V^5}{P n^2}}$.

η, Efficiency.

n, Revolutions per second, r. p. s.

Φ, Effective helix angle $= \tan^{-1}\left(\frac{V}{2\pi r n}\right)$

5. NUMERICAL RELATIONS

1 hp = 76.04 kg/m/s = 550 lb./ft./sec.
1 kg/m/s = 0.01315 hp
1 mi./hr. = 0.44704 m/s
1 m/s = 2.23693 mi./hr.

1 lb. = 0.4535924277 kg.
1 kg = 2.2046224 lb.
1 mi. = 1609.35 m = 5280 ft.
1 m = 3.2808333 ft.